7-7-2015

Design and Synthesis of New Inhibitors for DNA Methyltransferase

Haidong Feng
University of Connecticut - Storrs, haidong.feng@uconn.edu

Design and Synthesis of New Inhibitors for DNA Methyltransferase

Haidong Feng

B.S., China Pharmaceutical University, 2013

A Thesis

Submitted in Partial Fulfillment of the

Requirements for the Degree of

Master of Science

At the

University of Connecticut

2015

APPROVAL PAGE

Master of Science Thesis

Design and Synthesis of New Inhibitors for DNA Methyltransferase

Presented by

Haidong Feng, B.S.

Major Advisor_____
Prof. Dennis L. Wright

Associate Advisor_____
Prof. Amy C. Anderson

Associate Advisor_____
Prof. Mark W. Peczuh

University of Connecticut

2015

To My Parents

ACKNOWLEDGEMENTS

I met my advisor Dr. Dennis Wright two years ago when I first came to the U.S. I knew nothing about this totally different country at that time. I cannot speak English well and I did not have any friends here. I went to visit Dennis and asked him whether I could study and work in his lab. He accepted me and then the first question he asked me is that “Do you have any place to stay?” That is a funny question but I felt so warm in my heart because I was alone in the country that is 7,000 miles away from home.

I would like to appreciate everything Dennis has done for me. He gave me the opportunity to do what I wanted to do in chemistry and biology. He gave me a lot of help in academic, my future plan and life. He let me know if I want to succeed, I need to motivate myself. He gave me a lot of trust and confidence even though I was just a rookie. He is the best advisor I have met in my life.

I would also like to thank Dr. Amy Anderson for directing me in drug design. I would never forget what I have learned from her class on drug design. A special thanks to Dr. Mark W. Peczuh for his valuable time and suggestions during my dissertation defense.

I will give my great thanks to Dr. Michael VanHeyst (Big Mike). He was my first mentor in this lab and first American friend. It was from Mike that I learnt how to do chemistry. He taught me every experiment and skill with patience and encouraged me every time. Not only in academia but also in lives. He taught me how to watch football, and hockey games then pushed me to support Buffalo Bills and Pittsburgh Penguin. We also watched the World Cup of soccer, of course, and we both like the

Dutch. He taught me how to enjoy my American life here and let me know all the people in the world are the same.

I also have to thank Dr. Narendran G-Dayanandan, my Indian buddy. In my second year in the lab I was working with him and he gave me hundreds and thousands of help in chemistry and lives. We talked about everything including culture, politics, language and history. I have been enjoying every moment working with him.

I still need to thank Eric Falcone, Eric Scocchera, Dr. Santosh Keshipeddy and Alex. They all gave me countless help and make my life here easier.

I would like to express my heartfelt gratitude to my parents, my father Ming Feng and my mother Xirong Wang. It's never been easy to let their only child studying away from home. However they have always been giving me unselfish love and support. I cannot thank them enough for everything they did for me. This thesis is dedicated to my parents.

Table of Content

CHAPTER ONE
INTRODUCTION

General Information

Although phenotypes can be changed through converting the information of DNA sequence, epigenetic changing also can make it. The initial definition of epigenetic is “the interactions between genes and their products leading to the realization of the phenotype” by Waddington. However, now it evolves to become more precisely that changes that can lead to a heritable and stable phenotype happens on a chromosome without changing its DNA sequence [1]. Epigenetic modifications such as DNA methylation, histone methylation, and histone acetylation play spectacular roles in physical process in life [2]. For example, histone acetylation and methylation as well as DNA methylation have influences on gene expression and repression. Among all the epigenetic modifications, DNA methylation is most likely best known and has been regarded as an important target for drug design, especially in cancer drug development. Aberrant DNA methylation has been proved that is associated with unplanned silencing based on two distinct forms: hypomethylation and hypermethylation. Global hypomethylation has something to do with the development and progression of cancer through different mechanisms. Hypermethylation is one of the major DNA methylation modifications that repress transcriptions of promoter regions in cancer cells’ suppressor genes. DNA methylation is a significant factor in regulating mammalian cells’ life cycle. Alterations in DNA methylation patterns can promote tumorigenesis and predispose genes to mutational events.

DNA Methyltransferases

DNA methylation is catalyzed by DNA methyltransferases (DNMTs) using S-Adenosyl-L- Methionine (SAM) as the methyl group donor. As recently, mammalian methyltransferases are divided into DNMT1, DNMT3 and TRDMT1 in which the TRDMT1 was named DNMT2 and does not methylate DNA rather a $tRNA^{Asp}$ [1]. They have C-terminal catalytic domain and N-terminal regulatory domain [3]. DNMT3 is a *de novo* methyltransferase that is prevalent and expressed in embryonic stages and differentiated cells, which means it can effectively methylate unmethylated DNA, whereas DNMT1 can maintain DNA-methylation pattern during replication, which means it has a higher affinity for a hemimethylated DNA strands than the unmethylated ones just as the Fig.1 shows [4] [5]. However the sequence in catalytic sites of DNMT3A and DNMT3B shows a certain homology with DNMT1 [2].

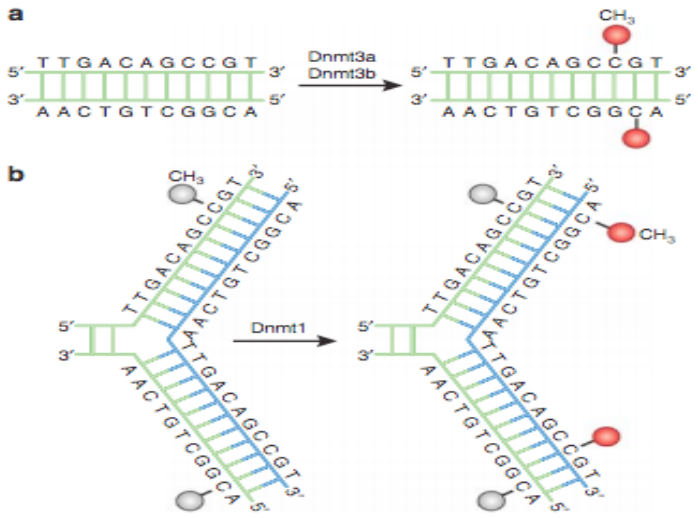

Figure.1 Scheme of DNA methylation. A. It is the action mode of DNMT3A/B. B. it is the action mode of DNMT1 Produced from Moore, L.D., T. Le, and G. Fan, *DNA methylation and its basic function.* Neuropsychopharmacology, 2013. **38**(1): p. 23-38.

Structure Analysis of DNA Methyltransferase 1 (DNMT1)

Here we focus more on DNMT1, which has proved its potency for drug target in cancer therapies. Mammal DNMT1 is a protein with 1616 amino acids whose structure can be divided into a regulatory domain and a catalytic domain. Motif IV includes the cysteine residue that can act as nucleophile attacking cytosine in the substrate and forming a transient covalent bond. Sequences at the N-terminus end named DMAP has been approved that has interactions with DNA methyltransferase associated protein-1 [6]. It usually helps bind DNA at CG sites [7]. In DNMT1, CXXC domain involves eight conserved cysteine residues clustered in two CXXCXXC repeat. This domain is essential for the catalytic activity for the enzyme [8]. It has been observed that the isolated fragment of C-terminal catalytic domain does not have any activities without N-terminal regulatory domain [7] [9]. BAH domains are Bromo-adjacent homology domains. These domains involved in transcriptional regulation are present in several proteins. Although its function roles in DNMT1 remain unclear, they have important role in protein-protein recognition and interaction in gene silencing [9].

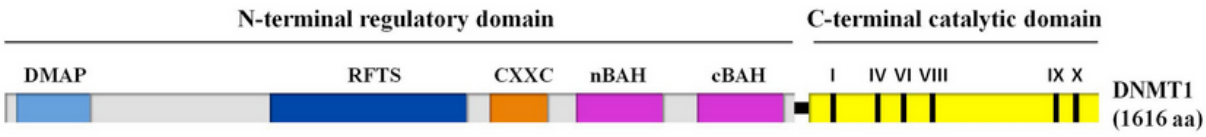

Figure.2 Primary structure of the DNMT1. Reproduced from http://www.frontiersin.org/files/Articles/132809/fgene-06-00090-r2/image_m/fgene-06-00090-g002.jpg

DNA Methlation in Cancer

In cancer cells, DNA methylation can lead to promoter hypermethylation at CpG islands and then silence tumor supprßessor genes [2]. Unlike mutagenic events, however, epigenetic mutations can be reversible. DNA demethylation of aberrantly silenced genes can recover gene expression [10]. In mammals, DNA methylation happens at the 5-position of cytosine in CpG dinucleotides and hypermethylation occurs in the CpG-rich sequences, which is called CpG island (regions with a high frequency of CpG sites). Gene expression can be manipulated through the action of repressor proteins that attach to silencing regions of the DNA. Because most CpG islands are involved in core promoters and transcription initiation, such as $p16^{INK4a}$ and *human mutL homologure*, the silence of genes can be triggered by hypermethylation because of poor recognition by transcription factors and recruitment of proteins, which are involved in the tumorigenic process [11]. Therefore, DNA methylation inhibitors are regarded as potential anticancer agents

Structure Analysis of Models from PDB

For now there is not any isolated human DNA methyltransferase crystal structures in free state available in Protein Data Bank (PDB). 3SWR and 3PTA are two complexes of human DNMT. 3SWR is structure of human DNMT1 in complex with Sinefungin and 3PTA is a crystal structure of human DNMT1 in complex with DNA. Both of them can be used to help design DNMT inhibitors. We found out that the sequence and tertiary structure of catalytic sites in mammal DNMT1 are conservative and the catalytic site is formed by two pockets, DNA binding pocket and

cofactor binding pocket are depicted in figure.3. According to the research [12] there are several residues of the DNMT playing important roles in catalyzing methylation process, which could be taken advantage of designing new inhibitors. For example, Arg174, Arg318, Glu128 and His321 in the catalytic site can form hydrogen bonds with pentose rings, phosphate group, amino group and 3'-hydroxy group of cytidine respectively. Glu128 and Arg174 could be involved into the catalytic mechanism through stabilizing the intermediate [13-15].

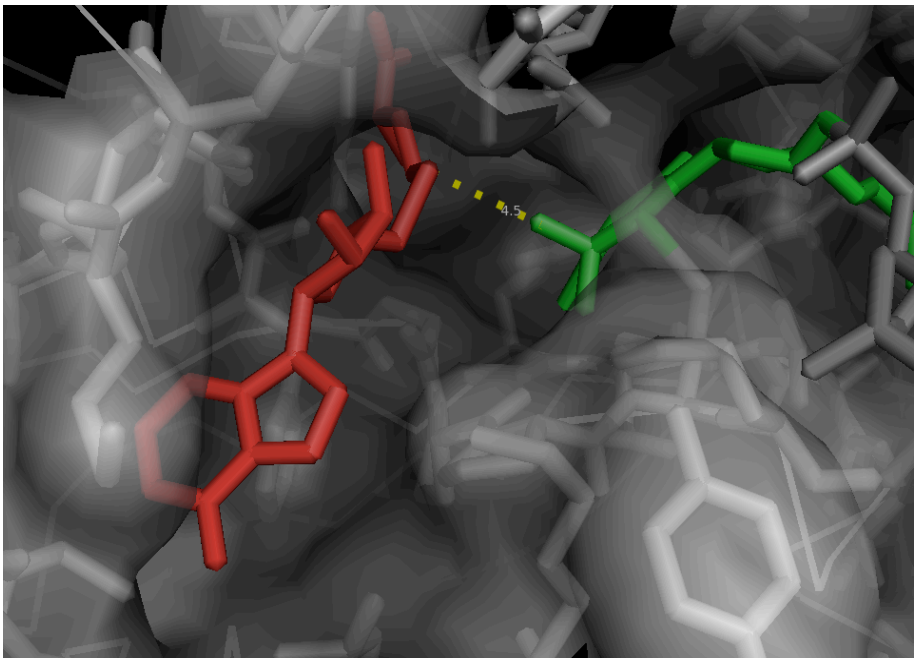

Figure.3 it shows the SAM (red) and Cytosine (green) in the catalytic site of DNMT1 (PDB: 4DA4). The position SAM occupies is cofactor pocket and the position Cytosine occupies is DNA pocket.

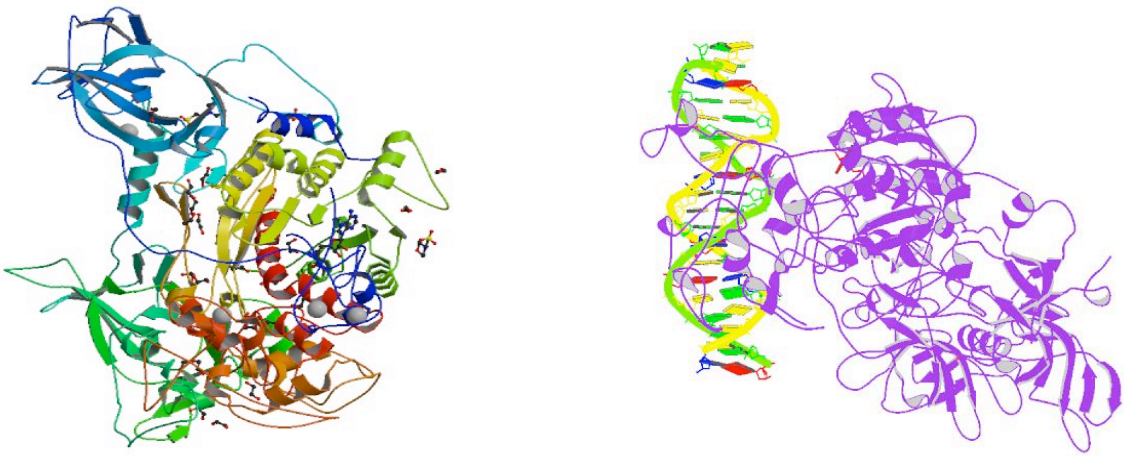

PDB: 3SWR PDB: 3PTA

Figure.4 3D structure of DNMT1 with different resourcesReproduced from http://www.rcsb.org/pdb/results/results.do?qrid=F05BBCF0&tabtoshow=Current

The Working Mechanism of DNMT1

The catalytic mechanism for the methylation of cytosine-5 has been discussed in detail several decades ago [16]. As depicted figure.5, a thiol group of the cysteine residue in the active site of DNMTs serves as a nucleophile that attacks the 6-position of cytosine to generate a covalent DNA-protein intermediate that possesses nucleophilic properties at the 5-position. This reactive intermediate accepts a methyl group from S-Adenosyl Methyionoine (SAM) to form a complex of 5-methyl covalent adduct and S-Adenosyl-L-Homocysteine (SAH). And the Glutamic acid in the active site is helpful for stabilizing the intermediate. Following the methyl transfer, a basic residue in the active site abstracts the proton at the 5-position and then the covalent bond formed between protein and thiol group was removed through ß- elimination to generate the methylated cytosine and the free enzyme [11].

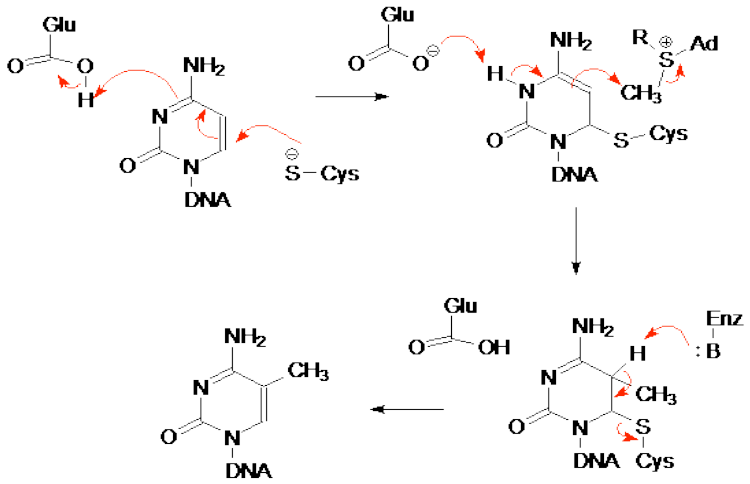

Figure.5 Scheme of catalytic process.
Reproduced from http://chemistry.umeche.maine.edu/CHY431/Nucleic/Methylation.gif

Inhibitors for DNMT1

Two types of methyltransferase inhibitors have been developed in last several decades, categorized into nucleoside analogue inhibitors and non-nucleoside analogue inhibitors.

Nucleoside inhibitors: In nucleoside inhibitor category, 5-azacytidine and 5-aza-2'-deoxycytidine have been approved by FDA for treating myelodysplastic syndrome (MDS), acute myeloid leukemia (AML), and chronic myelomonocytic leukemia (CMML) [17].

When nucleoside analogues are incorporated into DNA, for example 5-azacytidine and 5-aza-2'-deoxycytidine, they can become substrates of the DNA replication. Azacytosine can be recognized as cytosine, which is a natural substrate for binding DNA methyltransferase and the enzyme will start the methylation reaction. The nucleophilic attack of the thiol group from the catalytic cysteine residue of the

DNMT occurs at the C6 position of azacytosine and results in a covalent bond between substrate and enzyme.

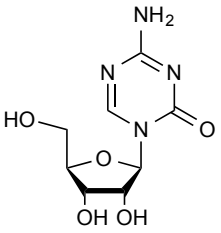

5-azacytidine

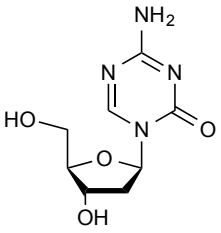

5-aza-2'-deoxycytidine

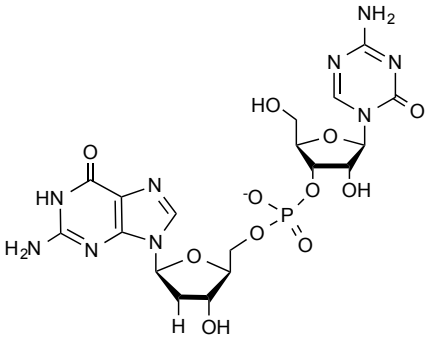

SGI-110

Figure.6: Nucleoside inhibitors of DNA methyltransferases

As demonstrated above, the covalent can be removed through a ß-elimination reaction then the DNMT can be released and recruited. However, because 5-azacytidine and 5-aza-2'-deoxycytidine have a nitrogen atom in place of the C-5 carbon atom, ß-elimination is blocked. As a result, the DNA methyltransferases remain bound to DNA as intermediates and the function of DNMT is blocked. In addition, covalently trapped DNMTs also compromises the functionality of DNA and

triggers DNA damage signaling, resulting in the degradation of trapped DNA methyltransferases [3, 4, 11, 18].

The most critical problems of 5-azacytidine and 5-aza-2'-deoxycytidine are toxic side effects and chemical instability. A great caution has been taken when using 5-azacytidine and 5-aza-2'-deoxycytidine at high doses. For many years, both drugs were administered at the maximum tolerated doses because health care providers believed that this would bring patients with the most benefit. Under this circumstance, however, both drugs can cause severe side effects. It has also been observed that the treatment of cultured cell lines with drug in the micromolar concentrations prolonged myelosuppression [19, 20]. The other biggest problem for azanucleoside inhibitors is chemical instability. In alkaline solutions, the 5-azacytosine ring of azanucleosides can be open and decomposed followed by losing inhibition activities. While in acidic solutions the glcosidic bond of azanucleosides is cleaved, which causes problems in oral administration. [4] As a result, modifications of those compounds have continuously implemented and improve plasma stability of azanucleosides. SGI-110 is one of the examples, which has a better chemical stability in vitro test and a improved resistance to enzymatic deamination [21].

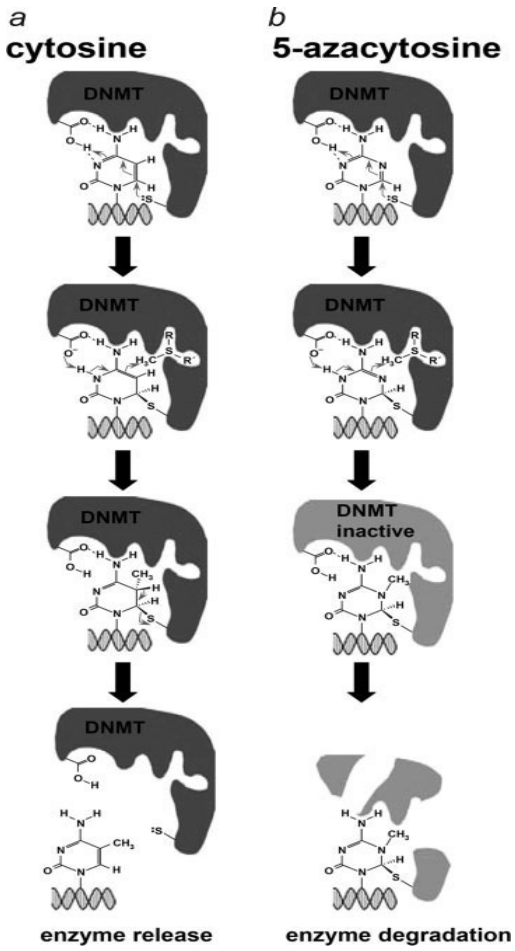

Figure.7 Trapping mechanism of azacytosine. (a) Normal mechanism of DNA methylation. (b) Mechanism-based inhibition of DNMTs by azacytosine containing DNA
Reproduced from Int. J. Cancer: 123, 8-13 (2008)

Non-nucleoside inhibitors: Because of the limitation in usage of nucleoside analogs in clinical treatment, a particular interests has recently emerged from non-nucleoside compounds, which exert their inhibitory effects through a variety of mechanisms instead of DNA incorporation. Among those compounds RG-108 [22] and SGI-1027 [23] are introduced.

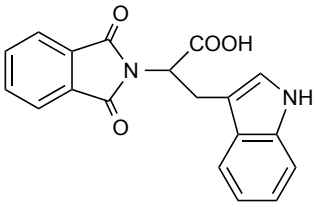

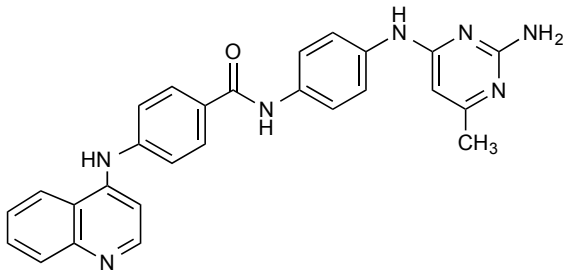

RG-108 SGI-1027

It has been approved that RG-108 has ability inhibition ability both in purified recombinant CpG methylase M.SssI and genomic DNA methylation level of human tumor cell line [6]. It occupies the same pocket of the native cytosine substrate. The research suggested that it is a mechanism-independent inhibitor because although it does not have a ring structure similar to cytosine it has carboxylate anion and carbonyl groups of phthalimide, which can form hydrogen bonds with Arginine and Cysteine respectively, preventing forming the covalent bond between substrate and catalytic cysteine [24]. RG-108 has approved its large range of utilities in inhibition. It can interact with human DNMT1 and the catalytic domain of murine DNMT3A [22]. SGI-1027 is a quinolone-based compound the study shows that it is a noncompetitive type and it probably competes with Ado-Met for access to the cofactor binding site of the enzyme. [25] According to the work of Jakyung Yoo and his colleagues [23] the quinolylamino benzamide group of SGI-1027 forms hydrogen bonds with many key amino acid residues at SAM binding pocket, such as Arg883, Arg887 and Glu660. The benzyl aminopyrimidine group of SGI-1027 occupies a region similar to the aminopurine ring of SAH. In addition, a benzene ring of both SGI-1027 and aminopruine ring of SAH makes π-π stacking interactions with enzyme. Researches

has shown the widely use of SGI-1027 in many varieties of human cancer cell lines. It shows comparable inhibitory activity of DNMT1, DNMT3A and DNMT3B without significant toxicity. It has been also suggested its selectivity in inhibiting DNMT1 when treating different mammal cancer cells. SGI-1027 can demethylate three different TSGs and then results in the reexpression of TSGs, which could be silenced due to the methylation of CpG islands in their promoters in human cancer cells [25].

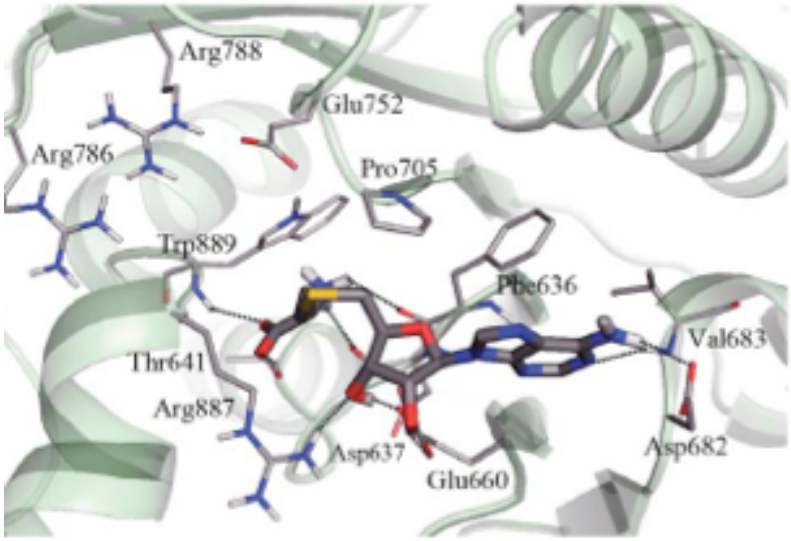

Figure.8 3D-interaction map displaying SGI-1027, SAH and human DNMT1 (PDB code: 3SWR)

Produced from Yoo, J., S. Choi, and J.L. Medina-Franco, *Molecular modeling studies of the novel inhibitors of DNA methyltransferases SGI-1027 and CBC12: implications for the mechanism of inhibition of DNMTs.* PLoS One, 2013. **8**(4): p. e62152.

Even though RG-108 and SGI-1027 can inhibit DNMTs directly, their details mechanism of action remain unknown. At present, there are no non-nucleoside DNMT inhibitors in medicine market or entering clinical trail. So it is therefore highly significant to develop new DNMT inhibitors.

References:

1. Gros, C., et al., *DNA methylation inhibitors in cancer: recent and future approaches.* Biochimie, 2012. **94**(11): p. 2280-96.
2. Chen, S., et al., *Identifying novel selective non-nucleoside DNA methyltransferase 1 inhibitors through docking-based virtual screening.* J Med Chem, 2014. **57**(21): p. 9028-41.
3. Song, J., et al., *Structure-based mechanistic insights into DNMT1-mediated maintenance DNA methylation.* Science, 2012. **335**(6069): p. 709-12.
4. Stresemann, C. and F. Lyko, *Modes of action of the DNA methyltransferase inhibitors azacytidine and decitabine.* Int J Cancer, 2008. **123**(1): p. 8-13.
5. Auclair, G. and M. Weber, *Mechanisms of DNA methylation and demethylation in mammals.* Biochimie, 2012. **94**(11): p. 2202-11.
6. Goll, M.G. and T.H. Bestor, *Eukaryotic cytosine methyltransferases.* Annu Rev Biochem, 2005. **74**: p. 481-514.
7. Fatemi, M., et al., *The activity of the murine DNA methyltransferase Dnmt1 is controlled by interaction of the catalytic domain with the N-terminal part of the enzyme leading to an allosteric activation of the enzyme after binding to methylated DNA.* J Mol Biol, 2001. **309**(5): p. 1189-99.
8. Pradhan, M., et al., *CXXC domain of human DNMT1 is essential for enzymatic activity.* Biochemistry, 2008. **47**(38): p. 10000-9.
9. Jurkowska, R.Z., T.P. Jurkowski, and A. Jeltsch, *Structure and function of mammalian DNA methyltransferases.* Chembiochem, 2011. **12**(2): p. 206-22.

10. Siedlecki, P., et al., *Discovery of two novel, small-molecule inhibitors of DNA methylation.* J Med Chem, 2006. **49**(2): p. 678-83.

11. Suzuki, T., et al., *Design, synthesis, inhibitory activity, and binding mode study of novel DNA methyltransferase 1 inhibitors.* Bioorg Med Chem Lett, 2010. **20**(3): p. 1124-7.

12. Singh, N., et al., *Molecular modeling and molecular dynamics studies of hydralazine with human DNA methyltransferase 1.* ChemMedChem, 2009. **4**(5): p. 792-9.

13. Jurkowski, T.P., et al., *Human DNMT2 methylates tRNA(Asp) molecules using a DNA methyltransferase-like catalytic mechanism.* RNA, 2008. **14**(8): p. 1663-70.

14. Kumar, S., et al., *DNA containing 4'-thio-2'-deoxycytidine inhibits methylation by HhaI methyltransferase.* Nucleic Acids Res, 1997. **25**(14): p. 2773-83.

15. Kuck, D., et al., *Novel and selective DNA methyltransferase inhibitors: Docking-based virtual screening and experimental evaluation.* Bioorg Med Chem, 2010. **18**(2): p. 822-9.

16. O'Gara, M., et al., *Enzymatic C5-cytosine methylation of DNA: mechanistic implications of new crystal structures for HhaL methyltransferase-DNA-AdoHcy complexes.* J Mol Biol, 1996. **261**(5): p. 634-45.

17. Egger, G., et al., *Epigenetics in human disease and prospects for epigenetic therapy.* Nature, 2004. **429**(6990): p. 457-63.

18. Valente, S., et al., *Selective non-nucleoside inhibitors of human DNA methyltransferases active in cancer including in cancer stem cells.* J Med Chem, 2014. **57**(3): p. 701-13.

19. Brueckner, B., D. Kuck, and F. Lyko, *DNA methyltransferase inhibitors for cancer therapy.* Cancer J, 2007. **13**(1): p. 17-22.

20. Zheng, Y.G., et al., *Chemical regulation of epigenetic modifications: opportunities for new cancer therapy.* Med Res Rev, 2008. **28**(5): p. 645-87.

21. Stach, D., et al., *Capillary electrophoretic analysis of genomic DNA methylation levels.* Nucleic Acids Res, 2003. **31**(2): p. E2.

22. Asgatay, S., et al., *Synthesis and evaluation of analogues of N-phthaloyl-l-tryptophan (RG108) as inhibitors of DNA methyltransferase 1.* J Med Chem, 2014. **57**(2): p. 421-34.

23. Yoo, J., S. Choi, and J.L. Medina-Franco, *Molecular modeling studies of the novel inhibitors of DNA methyltransferases SGI-1027 and CBC12: implications for the mechanism of inhibition of DNMTs.* PLoS One, 2013. **8**(4): p. e62152.

24. Li, E., C. Beard, and R. Jaenisch, *Role for DNA methylation in genomic imprinting.* Nature, 1993. **366**(6453): p. 362-5.

25. Datta, J., et al., *A new class of quinoline-based DNA hypomethylating agents reactivates tumor suppressor genes by blocking DNA methyltransferase 1 activity and inducing its degradation.* Cancer Res, 2009. **69**(10): p. 4277-85.

CHAPTER TWO
RESULTS AND DISCUSSION

Structure Analysis and Ligand Design

Structure guided ligand design was carried out by utilizing the crystal structure of murine DNMT1. The murine model (PDB code: 4DA4) depicts the active state of the methyl transfer reaction with the DNA substrate, SAH (byproduct of SAM after reaction) and the enzyme DNMT1. Though the crystal structure of the human DNMT1 in the active form is not available currently, the catalytic site is highly conserved in both murine and human models.[1]

The active site of DNMTs consists of two pockets namely the DNA binding pocket and SAM binding pocket. SAM binding pocket shows a high affinity for hydrophobic group and DNA binding pocket shows a hydrophilic character. According to the analysis of the crystal structure as well as the work from Shijie Chen and his colleagues [2], a good inhibitor occupies both the SAM and DNA binding pocket. Our goal is to design and synthesize an inhibitor that can mimic the ribose of the cytosine, which can be optimized later to occupy the SAM pocket. Our design of compound is based on the dibromoenone moiety. The versatility of the dibromoenone in terms of its functionality can be utilized to synthesize derivatives that can be either a nucleoside or a non- nucleoside inhibitor as shown in Figure.1

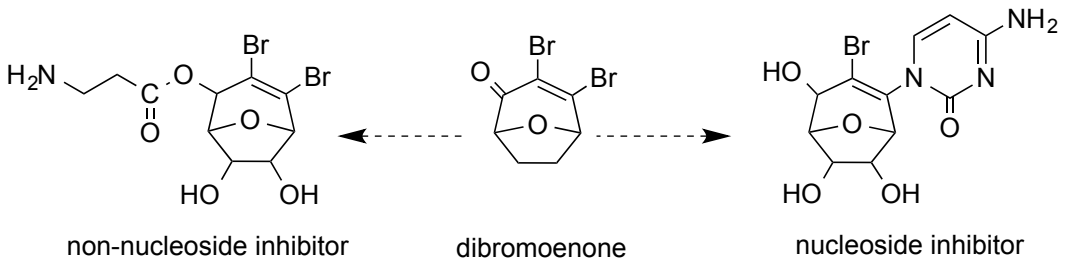

Figure.1 design strategy of inhibitors from dibromoenone

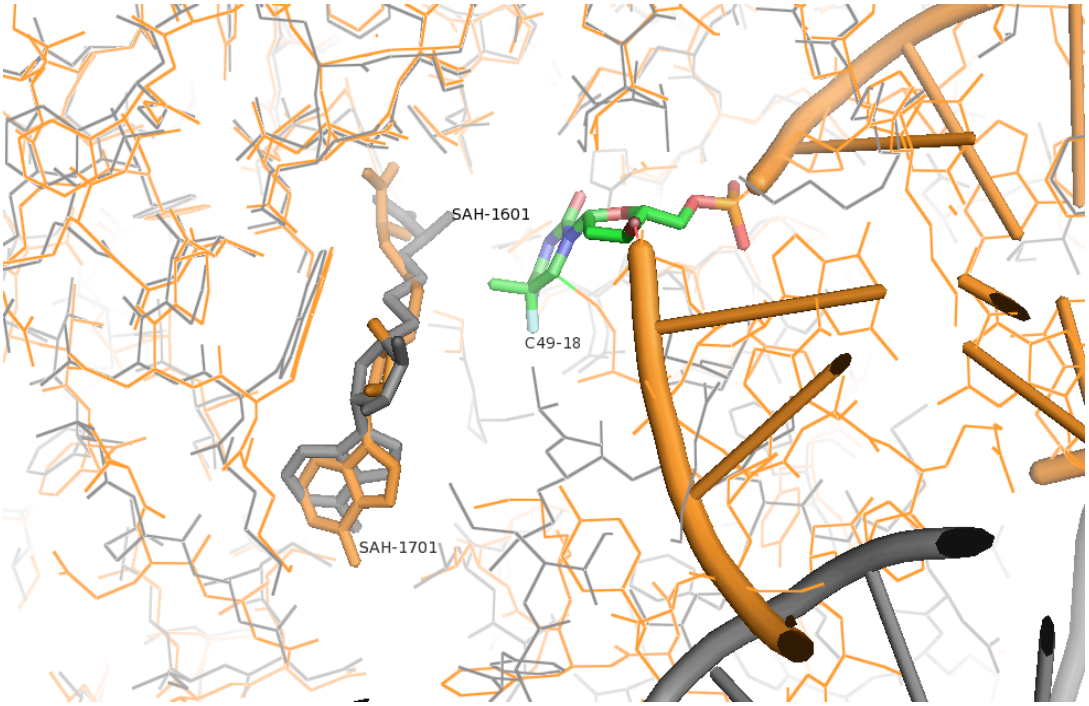

Figure.2 Superimposed models of human and murine DNMTs. Orange: murine DNMT1 (PDB code: 4DA4); Gray: human DNMT1 (PDB code: 3PTA). Difference in positions and poses of DNA substrate is shown.

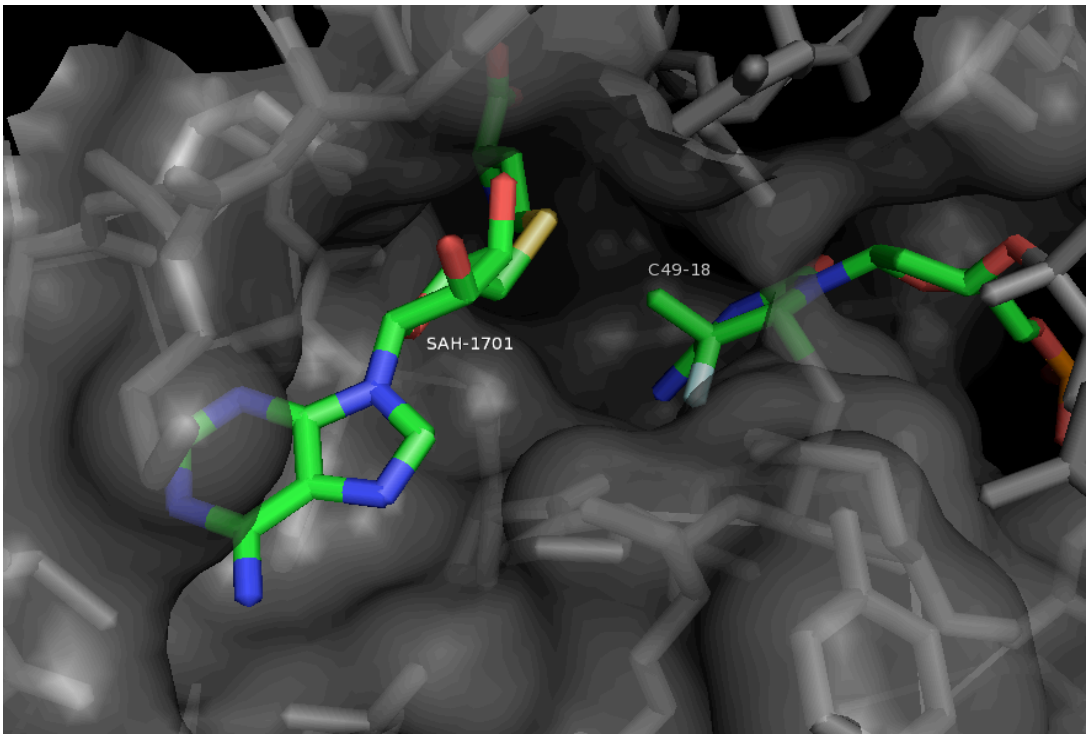

Figure.3 Binding pockets in DNA methyltransferase. SAH-1701 is at the SAM pocket and C49-18 is at the DNA pocket

Binding pocket of DNMT1

The residues those are common to the DNA pocket in Nanerder Singh's work [3] are Pro86, Cys88, Glu128, Arg172, Arg174, Thr320, His321, Gly440, Asn441 and Arg318. In Narender Singh's work, several hydrogen bonds were predicted between the inhibitors and enzyme. Arg174 (Arg1313 in 4DA4) can make several hydrogen bonds with oxygens in cytosine ring and phosphate group of the DNA substrate. Notably, the intermediate formed after the nucleophilic attack of AdoMet can be stabilized through interactions between carbonyl oxygen of the cytosine ring and two residues - Arg174, Arg318 (Arg1315 in 4DA4). The hydrogen bond between Glu128 (Glu1269 in 4DA4) and the amino group of the cytosine ring is also very important. It can be predicted that Pro1227 can form interaction with amino group of cytosine ring

as shown in Figure.5 In addition, His321 (Thr1530 in 4DA4) can make a hydrogen bond with 3'-hydroxy group.

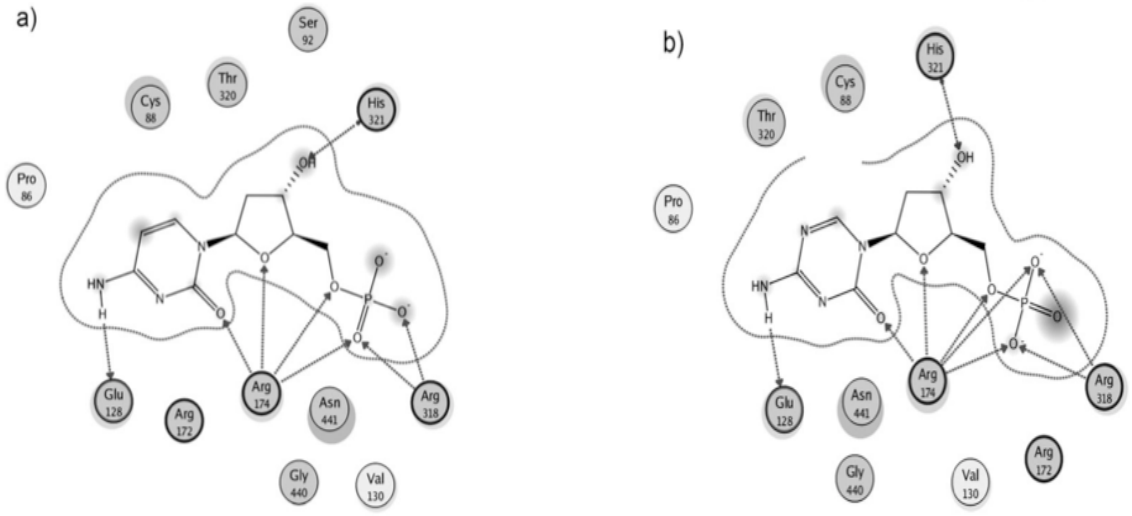

Firgure.4 2D-interaction map displaying amino acid residues with a) 2'-deoxycytidine and b) 5-aza-2'-dexoycytidine. Produced from Singh, N., et al., *Molecular modeling and molecular dynamics studies of hydralazine with human DNA methyltransferase 1.* ChemMedChem, 2009. **4**(5): p. 792-9.

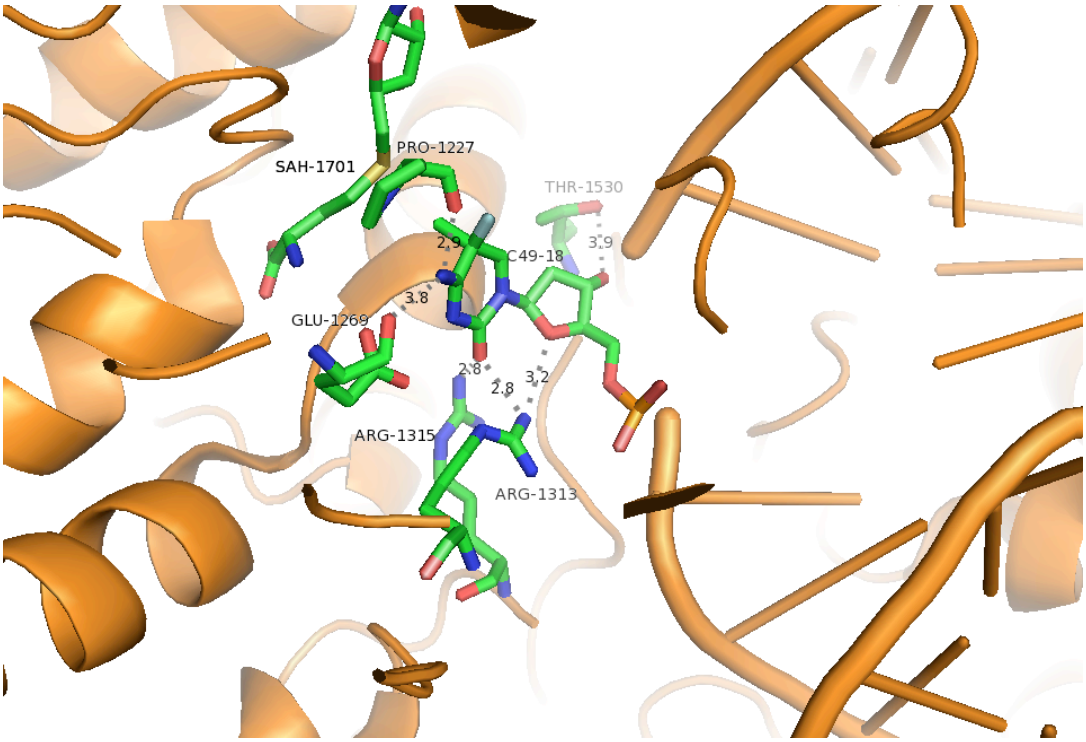

Figure.5 3D-interaction map displaying key amino acid residues with cytidine substrate.

Glu1269, Arg1313 and Arg1315 in PDB model 4DA4 are conserved across the mammalian models in the active site. These amino acids residues are essential for maintaining and stabilizing the binding position between flipped-out target cytidine and enzyme, and/or they could play roles in chemical reactions directly.

Of the three residues, Glu1269 plays a pivotal role during the catalytic process. This was confirmed by a mutation experiment for Glu1269 and Arg1315.[4] The mutation results in several fold loss of catalytic activity. This could be explained by the loss of hydrogen bonding between Glu1269 and cytosine N3, which plays an important role at the reactant and at the transition state. It can build a hydrogen bond with cytosine N3 so the proton would vibrate between being bonded to Glu1269 and to cytosine N3, which would stabilize the transition state.

Although hydrogen bond between Arg1313, Arg1315 in PDB model 4DA4 and cytosine O2 and O4' are weak in reactant, transition and intermediate, they indeed maintain hydrogen bonds through stabilizing electrostatic interaction from near-hydrogen bonding orientations in all states. [4] These results can provide meaningful information for future design of inhibitors.

Because a big region of SAM binding pocket is relatively hydrophobic, a prediction can be made that the compounds we made will bind at the DNA binding pocket, which is more hydrophilic. Compound **15** docking result is shown in figure.5. It can bind at the position as the same as where cytosine was. It can build hydrogen bonds with most of the key amino acid residues in active site, such as Arg1313, Arg1315, Glu1269, Pro1227 and Asn1580. Compound **15** are so close to Glu1269 that a strong hydrogen bond can be formed, which could make compound **15** to be

more competitive. At the same time interactions between arginines and compound **15** are stronger than that between argnines and cytidine substrate. In addition, the hydrogen bond formed between Asn1580 and compound **15** can be helpful for stabilizing this intermediate, which is not available in the natural catalytic process. According to the SYBYL docking results of compound **15**, it occupies the DNA pocket with a good affinity, as a result, compound **15** probably will compete with DNA substrate when binding to the enzyme during the catalytic process.

a)

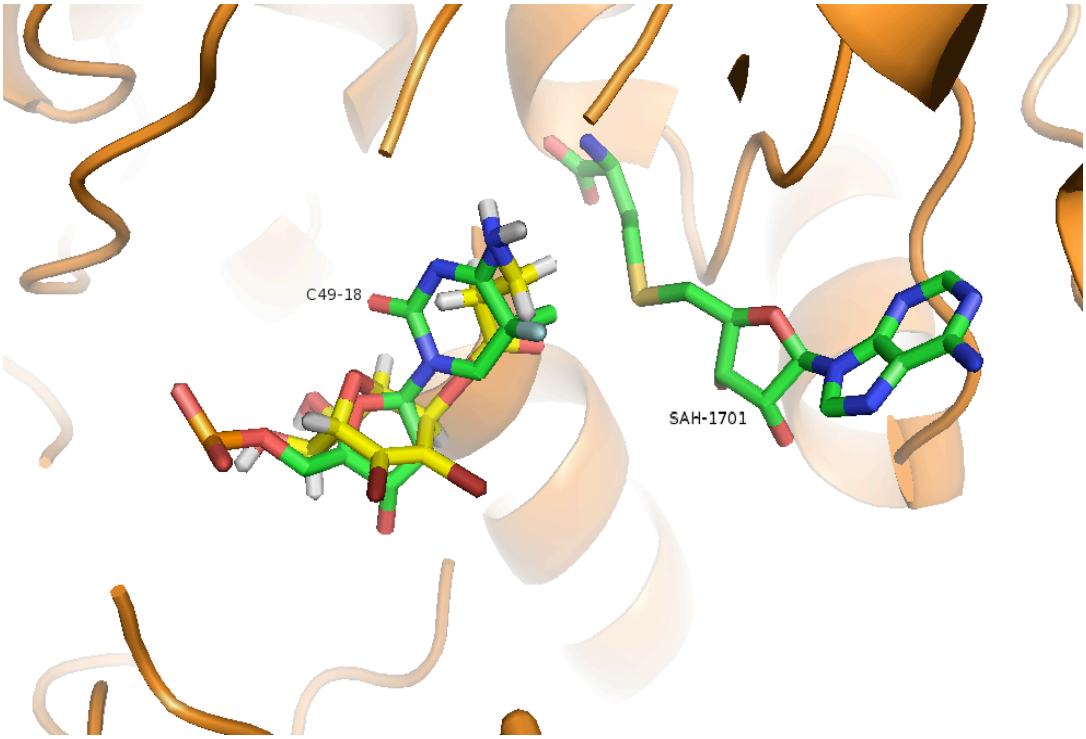

b)

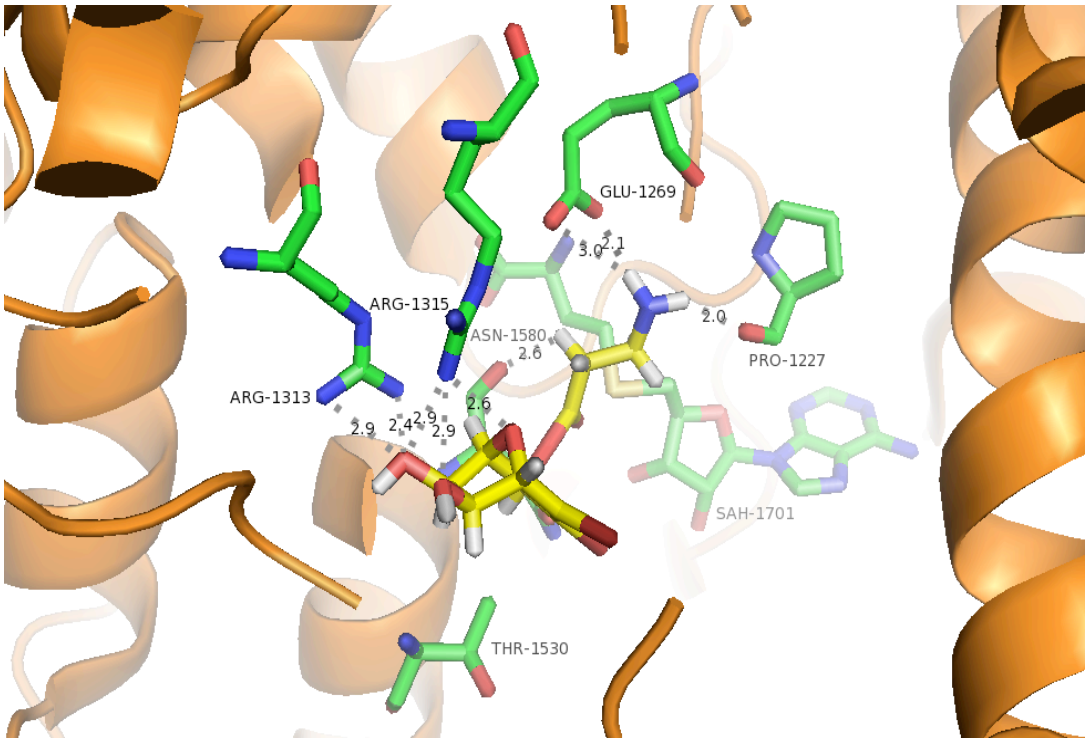

Figure.6 SYBYL docking results. a) superimposed model of (R)-Exo-**15** and Cytidine. (Green: Cytidine; Yellow: (R)-Exo-**15**). b) 3D-interaction map showing key amino acid residues with (R)-Exo-**15** (Green: residues from enzyme)

Because compound **15** is closer to these key amino acid residues, it can be predicted that it has a higher affinity than the natural DNA substrate and can provide inhibitory activity. Compound **18** was designed to determine the effect of removing one carbon from amino acid side chain of compound **15.**

Experiment Results

In the past several decades, many nucleoside analogs and non-nucleoside analog DNMTi have been developed.[5] However they all have some disadvantages, for example, toxicity, low sensitivity and low selectivity. A new series of compounds are being developed based on 8-oxabicyclo [3.2.1] octane nucleus and

dibromoenone, which have found wide application for natural products and other important compounds. [6, 7]

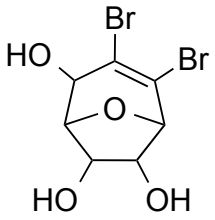

3,4-dibromo-8-oxabicyclo[3.2.1]oct-3-ene-2,6,7-triol

Scheme 1: retrosynthetic analysis

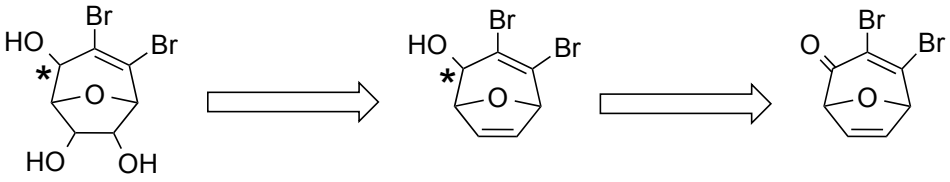

3,4-dibromo-8-oxabicyclo [3.2.1]oct-3-ene-2,6,7-triol

3,4-dibromo-8-oxabicyclo [3.2.1]octa-3,6-dien-2-ol

dibromoenone

For designing DNMT inhibitors, we chose 3,4-dibromo-8-oxabicyclo[3.2.1]oct-3-ene-2,6,7-triol as the core of the pharmacophore. The Scheme 1 shows the retrosynthetic analysis of synthesizing the compounds. The reasoning behind the selection of this moiety is to mimic the ribose of the cytidine molecule. In order to elucidate the activity of the 4 diastereomers , CBS resolution of the dibromoenone was carried out to separate the diastereomers and dihydroxylated using OsO_4 and NMO. Since the biological activity was exhibited only by (S)-diastereomers, newer compounds would be synthesized based on these diasteroemers – **1**&**2**.

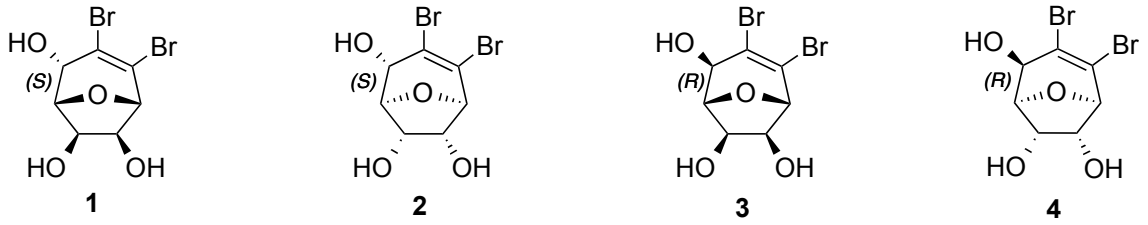

Initially racemic derivatives of 3,4-dibromo-8-oxabicyclo[3.2.1]oct-3-ene-2,6,7-triol were synthesized to understand the biological profile. The target product **15** is designed according to the structure of the active sites in DNMTs. Our retrosynthetic strategy targeted intermediate **14,** containing the intact pharmacophore with a Boc-protection on amine group. The intermediate **14** was thought to arise from the dihydroxylation of intermediate **13**, which was a result compound from the esterification between dibromoenone alcohol and a Beta-amino acid, Boc-ß-Ala-OH. Diastereomers of dibromoenone alchols could be synthesized from dibromoenone using the method developed by VanHeyst et al [8]

Scheme 2: retrosynthetic analysis

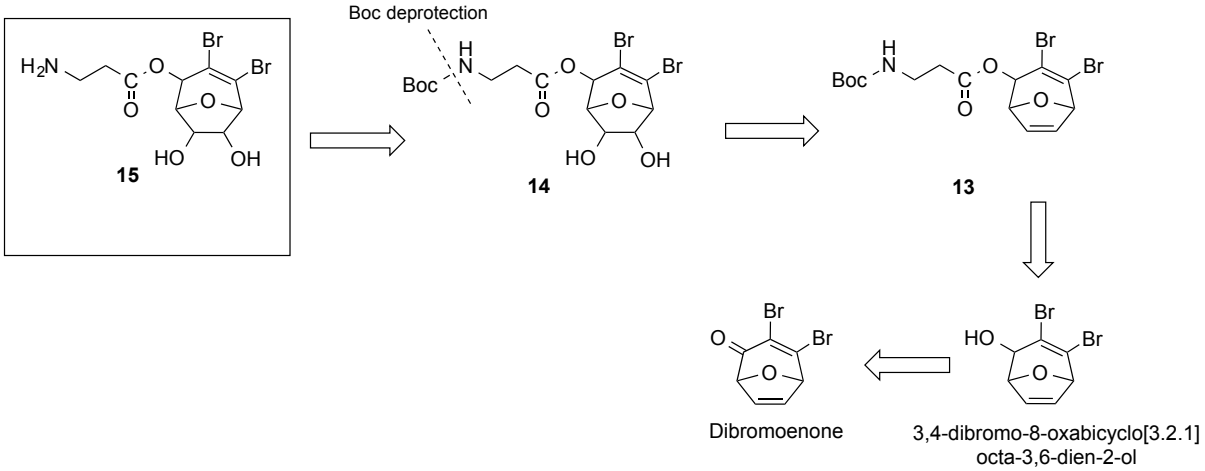

The reduced product of dibromoenone was obtained using sodium borohydride with 95% yields. [9]

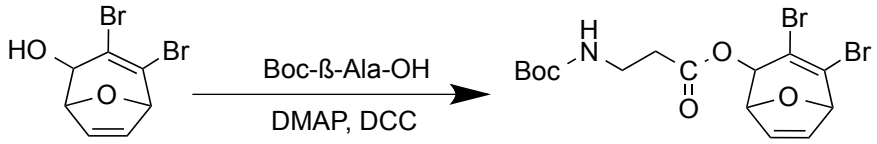

3,4-dibromo-8-oxabicyclo [3.2.1]octa-3,6-dien-2-ol

13

The esterification between dibromoenone and Boc-ß-Ala-OH is one of the key steps in the whole synthesis. At the beginning, Yumiko Yamand's procedure was employed in a Mukaiyama condition.[10] The long reaction time and low yields led to the use of Philipp Barbie's esterification reaction in DMAP and DCC.[11] This method generated 13 in good yields overnight.

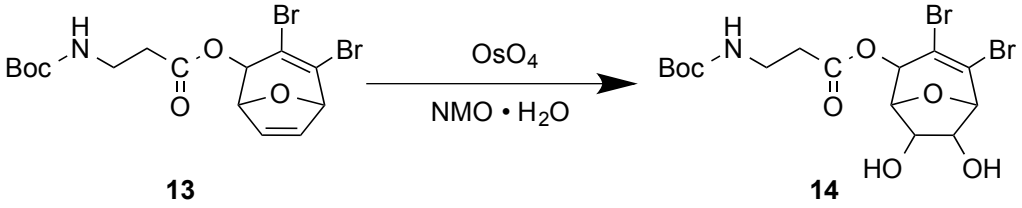

13 **14**

13 underwent dihydroxylation with OsO4 and NMO. The dihydroxylated product 14 was sensitive to silica gel during column resulting in the cleavage of the side chain. Hence the product was isolated and taken to the next step of deprotection. The reason of the phenomenon is still not clear but probably because that the secondary amine group could be as a nucleophilie attacking ester bond and then form a 4 membered ring or secondary alcohols would attack ester bond and then form a 6 members ring in acidic condition. As a result of both reasons above, the side chain would be cleaved and product was destroyed. On the contrary, there was no

problem when using Fluorenylmethyloxycarbonyl (Fmoc) group as protection group. Maybe Fmoc group hindered the amine group from reaching ester bond so that it could not form a stable 6 members ring.

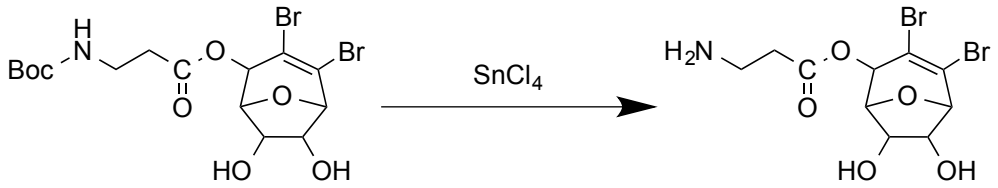

14 **15**

The traditional method of Boc deprotection using trifluoroacetic acid at 1, 7,14 and 25 equivalent was carried out at low temperature. [12] The same problem of side-chain cleavage associated with column purification was observed with this deprotection strategy. When ZnBr2 was used no reaction took place. Finally a milder method of Boc-deprotection published by Robert Frank and Mike Schutkowski was employed.[13] The compound **14** could be deprotected within 3h at the room temperature using $SnCl_4$. The resulting oil could be dissolved in methanol and the crude product precipitated by adding diethyl ether. Because the impurities were also polar and compound **15** was still sensitive to the acidic condition, a pure compound was obtained after triturating with ethyl acetate and methanol.

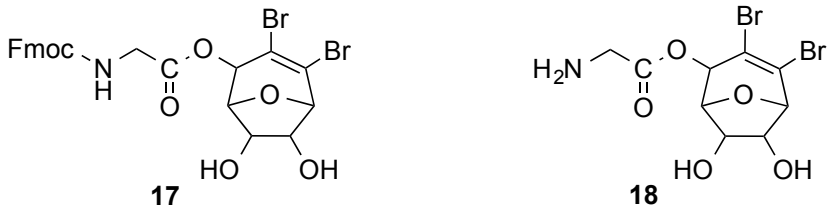

17 **18**

Compound 17 was obtained by the esterification of the alcohol with Fmoc glycine. The deprotection method using piperidine in DMF gave the product which needs to be purified for further characterization and biological testing.

In conclusion, we have designed and synthesized a new non-nucleoside DNMT inhibitor based on dibromoenone. According to the SAR analysis, several key amino acid residues have been defined and taken advantage of for designing DNMT inhibitors. Future biolgical evaluations of these dibromotrialcohol series might help in building lead compounds.

References:

1. Asgatay, S., et al., *Synthesis and evaluation of analogues of N-phthaloyl-l-tryptophan (RG108) as inhibitors of DNA methyltransferase 1.* J Med Chem, 2014. **57**(2): p. 421-34.
2. Chen, S., et al., *Identifying Novel Selective Non-Nucleoside DNA Methyltransferase 1 Inhibitors through Docking-Based Virtual Screening.* Journal of Medicinal Chemistry, 2014. **57**(21): p. 9028-9041.
3. Singh, N., et al., *Molecular modeling and molecular dynamics studies of hydralazine with human DNA methyltransferase 1.* ChemMedChem, 2009. **4**(5): p. 792-9.
4. Yang, J., et al., *DNA cytosine methylation: structural and thermodynamic characterization of the epigenetic marking mechanism.* Biochemistry, 2013. **52**(16): p. 2828-38.
5. Gros, C., et al., *DNA methylation inhibitors in cancer: recent and future approaches.* Biochimie, 2012. **94**(11): p. 2280-96.
6. Orugunty, R.S., et al., *Bridged synthons from tetrabromocyclopropene: studies on the rearrangement of the primary Diels-Alder adduct with 2,5-dimethylfuran.* J Org Chem, 2004. **69**(2): p. 570-2.
7. Orugunty, R.S., et al., *Silver-promoted reactions of bicyclo[3.2.1]octadiene derivatives.* Org Lett, 2002. **4**(12): p. 1997-2000.
8. VanHeyst, M.D., E.Z. Oblak, and D.L. Wright, *Stereodivergent resolution of oxabicyclic ketones: preparation of key intermediates for platensimycin and other natural products.* J Org Chem, 2013. **78**(20): p. 10555-9.

9. Joshi, M.V. and C.S. Narasimhan, *Catalysis by heteropolyacids: Some new aspects.* Journal of Catalysis, 1989. **120**(1): p. 282-286.

10. Yamano, Y., et al., *Lipophilic amines as potent inhibitors of N-acylethanolamine-hydrolyzing acid amidase.* Bioorg Med Chem, 2012. **20**(11): p. 3658-65.

11. Barbie, P., et al., *Stereoselective synthesis of deuterium-labeled (2S)-cyclohexenyl alanines, biosynthetic intermediates of cinnabaramide.* Org Lett, 2012. **14**(23): p. 6064-7.

12. Han, G., M. Tamaki, and V.J. Hruby, *Fast, efficient and selective deprotection of the tert-butoxycarbonyl (Boc) group using HCl/dioxane (4 m).* The Journal of Peptide Research, 2001. **58**(4): p. 338-341.

13. Frank, R. and M. Schutkowski, *Extremely mild reagent for Boc deprotection applicable to the synthesis of peptides with thioamide linkages.* Chemical Communications, 1996(22): p. 2509-2510.

CHAPTER THREE
EXPERIMENTS

General procedures: All reactions were carried out under an inert argon atmosphere with dry solvent under anhydrous conditions unless otherwise stated. Commercial grade reagents and solvents were used without further purification except as indicated below. Hexanes, tetrahydrofuran (THF), diethyl ether (Et_2O), and dichloromethane (CH_2Cl_2) were used directly from a Baker cycle-tainer system. Reagents were purchased at the highest commercial quality and used without further purification, unless otherwise noted. Yields refer to chromatographically and spectroscopically (^1H NMR) homogenous materials, unless otherwise stated. Reactions were monitored by thin layer chromatography (TLC) carried out on Wharman silica 60 Å precoated plates using UV light as the visualizing agent and an acidic mixture of anisaldehyde or basic aqueous potassium permanganate ($KMnO_4$) and heated as developing agents. Flash chromatography was performed using Baker silica gel (60Å particle size). NMR spectra were recorded on Bruker-500 and 400 instruments and calibrated suing residual undeuterated solvent as internal reference ($CHCl_3$ at δ 7.27 ppm ^1H NMR, δ 77.0 ppm ^{13}C NMR). The following abbreviations ere used to explain the multiplicities: s = singlet, d = doublet, t = triplet, q = quartet, m = multiplet, b = broad. High-resolution mass spectra (HRMS) were obtained from the University of Connecticut Special Facility by electrospray ionization of flight reflectron experiments.

Experimental Procedures:

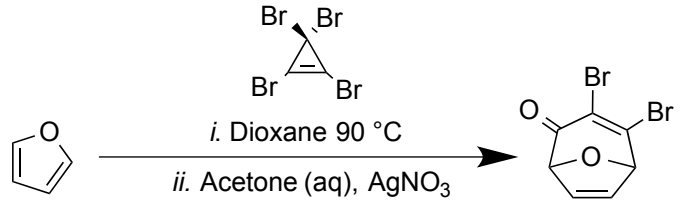

furan dibromoenone

General procedure for one-pot Diels Alder and silver hydrolysis: To a flame dried pressure vessel was added furan (110 mmol) and solvate with 1,4-dioxane (24 mL). The solution was treated with freshly distilled TBCP (38.9 g, 110 mmol) at r.t then the vessel was sealed. The vessel was stirred overnight at r.t before gradually heated to 80 °C and held at that temperature until all starting material was consumed in about 2h. After this time, the reaction was allowed to cool to r.t, diluted with acetone (224 mL) and treated with 2 equivalent $AgNO_3$ (aq) (37 g, 220 mmol in 122 mL of H_2O) over 20 min. The suspension was allowed to stir at r.t for 3h before being poured over solid $NaHCO_3$ (37 g, 440 mmol) slowly. The solids were removed by filtration through Celite and washed with acetone with acetone (300 mL). The filtrate was concentrated and then extracted with Et_2O (4 x 100 mL). The combined organic layers were washed with sat. $NaHCO_3$ (2 x 100 mL), H_2O (3 x 100 mL), brine (2 x 100 mL) dried over sodium sulfate and concentrated. The resulting crude dibromoenone was purified by flash chromatography using 25 % EtOAc in hexanes as the eluent to afford products as yellow solids. The spectral data of it was consistent to previous work done in the lab. Yield is 94mmol (85%)

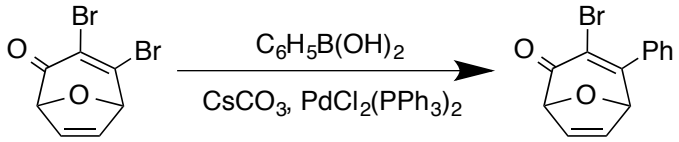

dibromoenone

3-bromo-4-phenyl-8-oxabicyclo [3.2.1]octa-3,6-dien-2-one

General procedure for Suzuki Coupling: To a flask starting material (0.286 mmol, 80 mg) and phenylboronic acid (0.457 mmol, 55.72 mg) were added in a solution system (0.2 M; THF, 1.3 mL; H_2O, 0.13 mL) under the inert argon atmosphere followed by adding $CsCO_3$. The solution was stirred at r.t for 15 minutes at which time $PdCl_2(PPh_3)_2$ was added. Following the consumption of all starting material the reaction was quenched with brine. The crude reaction mixture was extracted using EtOAc (3 x 25 mL) then washed with brine and dried over sodium sulfate. The resulting crude compound was separated from impurities through the flash chromatography using 10 % EtOAc in hexanes. Yield is 0.1mmol (35%).

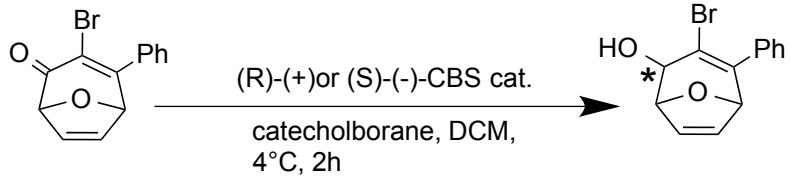

3-bromo-4-phenyl-8-oxabicyclo [3.2.1]octa-3,6-dien-2-one

3-bromo-4-phenyl-8-oxabicyclo [3.2.1]octa-3,6-dien-2-ol

General procedure for CBS reduction: To a flame dried flask was added substrate in CH_2Cl_2 (0.3 M) followed by adding (R)-(+) or (S)-(-)-CBS catalyst (50 mol%). The solution was stirred at r.t for about 20 minutes at which time the reaction was cooled down to 4 °C and then catecholborane (150 mol%) was added. After the consumption of all starting material, the reaction was quenched with 15 % NaOH and

allowed to stir at r.t for 1h. The aqueous layer was extracted with CH_2Cl_2 (3 x 0.05M). The combined organic layers were washed with 15% NaOH (3 x 0.05 M) water and birne, dried over sodium sulfate and concentrated. The resulting diastereomers were separated and purified by flash chromatography (SiO_2, 1:200 g) using 5% EtOAc in hexanes as the eluent to afford products as white solids.

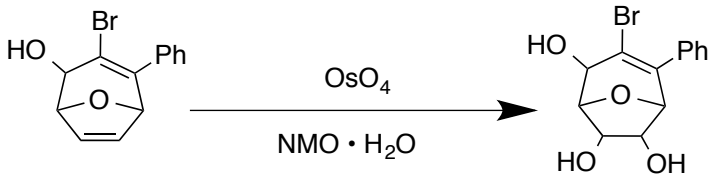

3,4-dibromo-8-oxabicyclo [3.2.1]octa-3,6-dien-2-ol

3-bromo-4-phenyl-8-oxabicyclo [3.2.1]oct-3-ene-2,6,7-triol

General procedure for Dihydroxylation: To a flask was added starting material (0.71 mmol, 200 mg) in solution (7.1 mL; Acetone, 5.68 mL; H_2O, 1.42 mL) followed by NMO • H_2O (4-Methylmorpholine N-Oxidate Monohydrate, 1.77 mmol, 239.25 mg). The solution was stirred at r.t for 15 minutes then OsO4 (0.0426 mmol, 0.271 mL) was added. After the consumption of all starting material, the reaction was quenched with water. Acetone in solution was removed by vacuum then the aqueous layer was extracted with EtOAc (3 x 25 mL). All organic layers were combined and washed with brine (100 mL) then dried over sodium sulfate and concentrated. The resulting crude compound was separated from impurities through the flash chromatography using 25 % EtOAc in hexanes.

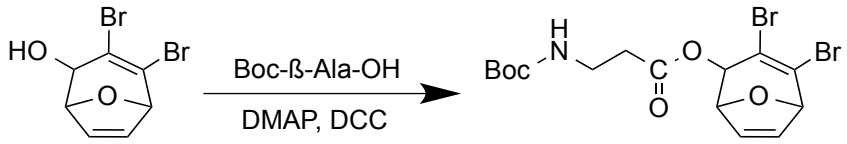

3,4-dibromo-8-oxabicyclo [3.2.1]octa-3,6-dien-2-ol

13

General procedure for esterification: To a flask the substrate (0.142 mmol, 40 mg) and Boc-ß-Ala-OH (0.142 mmol, 26.87 mg) were added in solution (0.16M Et_2O, 0.9 mL). DMAP was added to the flask then solution was stirred until it became into clear, at which time the solution was cooled to 0 °C for 10 minutes then added DCC and the solution was allowed to warm to r.t and leave it overnight. Following the consumption of all starting materials the suspension was filtered and filtrate was washed with sat. sodium bicarbonate (3 x 25 mL) and brine (25 mL) then dried over sodium sulfate and concentrated. The resulting crude compound was purified using flash chromatography with 10% EtOAc in hexanes.

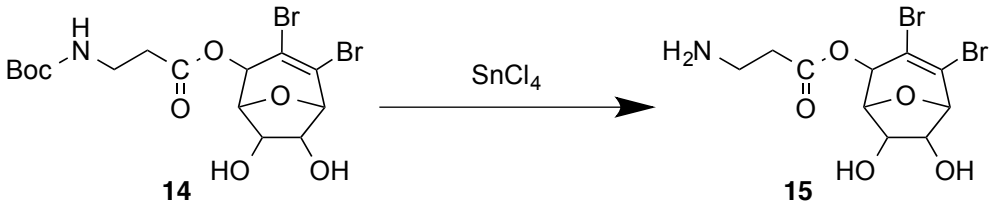

14 **15**

Procedure for Boc Deprotection: The stirring solution of starting material (0.037mmol, 18mg) in EtOAc, the $SnCl_4$ (0.074mmol, 0.074mL) was added at r.t. The resulting solution turning from clear into cloudy was stirred until TLC analysis showed all starting material has been consumed after 3 hours. Then the solvent was evaporated in vacuum and the remaining oil dissolved in methanol and the product

precipitated after adding diethyl ether. The solid was washed with diethyl ether twice and dried in the vacuum. The crude product was recrystallized by the solvent system of acetyl acetate-hexane, yielding 7.35mg, 0.019mmol (50%)

(1R,2S,5S,6S,7R)-3,4-dibromo-8-oxabicyclo[3.2.1]oct-3-ene-2,6,7-triol

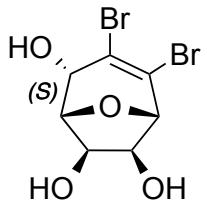

1

^{1}H NMR (500 MHz, DMSO-d_6) δ 6.15 (s, 1H), 5.17 (s, 1H), 5.07 (s, 1H), 4.52 (d, *J* = 6.2 Hz, 1H), 4.42 (s, 1H), 4.34 (s, 1H), 4.16 (d, *J* = 5.6 Hz, 1H), 4.03 (d, *J* = 6.1 Hz, 1H).^{13}C NMR (126 MHz, MeOD) δ 141.62, 137.08, 128.19, 128.16, 128.02, 122.97, 86.47, 86.42, 73.33, 70.29, 69.23; HRMS (DART) calcd for $C_7H_8Br_2O_4$ $[M+H]^+$: 314.8868

(1S,2S,5R,6R,7S)-3,4-dibromo-8-oxabicyclo[3.2.1]oct-3-ene-2,6,7-triol

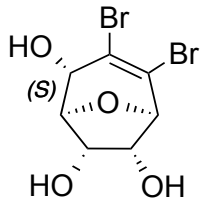

2

^{1}H NMR (500 MHz, DMSO-d_6) δ 5.97 (d, *J* = 7.5 Hz, 1H), 5.24 (s, 1H), 5.03 (d, *J* = 5.9 Hz, 1H), 4.42 (s, 1H), 4.06 (s, 1H), 4.03 (d, *J* = 6.0 Hz, 1H), 3.99 (d, *J* = 4.0 Hz, 1H), 3.83 (d, *J* = 7.0 Hz, 1H).^{13}C NMR (126 MHz, MeOD) δ 125.96, 123.33, 88.27, 86.84, 73.36, 72.47, 71.54. HRMS (DART) calcd for $C_7H_8Br_2O_4$ $[M+NH_4]^+$: 333.9113

(1R,2R,5S,6S,7R)-3,4-dibromo-8-oxabicyclo[3.2.1]oct-3-ene-2,6,7-triol

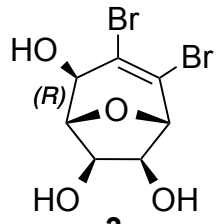

3

^{1}H NMR (500 MHz, DMSO-d_6) δ 5.97 (dd, *J* = 7.8, 2.9 Hz, 1H), 5.23 (d, *J* = 5.3 Hz, 1H), 5.02 (d, *J* = 6.0 Hz, 1H), 4.41 (s, 1H), 4.06 (d, *J* = 3.4 Hz, 1H), 4.02 (t, *J* = 6.3 Hz, 1H), 3.98 (t, *J* = 5.6 Hz, 1H), 3.82 (dd, *J* = 8.0, 1.5 Hz, 1H).^{13}C NMR (126 MHz, MeOD) δ 125.96, 123.33, 88.27, 86.84, 73.36, 72.47, 71.54. HRMS (DART) calcd for $C_7H_8Br_2O_4$ $[M+NH_4]^+$: 333.9113

(1S,2R,5R,6R,7S)-3,4-dibromo-8-oxabicyclo[3.2.1]oct-3-ene-2,6,7-triol

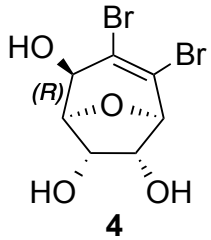

4

^{1}H NMR (500 MHz, DMSO-d_6) δ 6.15 (d, *J* = 6.7 Hz, 1H), 5.16 (d, *J* = 5.3 Hz, 1H), 5.06 (d, *J* = 6.9 Hz, 1H), 4.52 (t, *J* = 6.6 Hz, 1H), 4.41 (t, *J* = 6.1 Hz, 1H), 4.34 (s, 1H), 4.16 (d, *J* = 5.6 Hz, 1H), 4.03 (t, *J* = 5.8 Hz, 1H).^{13}C NMR (126 MHz, MeOD) δ 127.12, 123.34, 87.53, 86.22, 73.07, 70.34, 69.97. HRMS (DART) calcd for $C_7H_8Br_2O_4$ $[M+H]^+$: 314.8868

(1R,2S,5S)-3-bromo-4-phenyl-8-oxabicyclo[3.2.1]octa-3,6-dien-2-ol

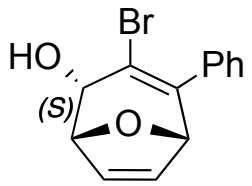

5

^{1}H NMR (500 MHz, Chloroform-*d*) δ 7.49 – 7.33 (m, 5H), 6.90 (dd, *J* = 6.0, 1.7 Hz, 1H), 6.34 (dd, *J* = 5.9, 1.8 Hz, 1H), 5.33 (dd, *J* = 6.1, 1.9 Hz, 1H), 4.98 (d, *J* = 1.7 Hz, 1H), 4.65 (t, *J* = 5.3 Hz, 1H), 2.21 (d, *J* = 5.0 Hz, 1H).^{13}C NMR (126 MHz, $CDCl_3$) δ 146.53, 140.81, 136.51, 129.30, 128.51, 127.84, 121.61, 83.13, 81.78, 67.93, 29.72. HRMS (DART) calcd for $C_{13}H_{11}BrO_2$ $[M\text{-}OH]^+$: 260.9915

(1S,2S,5R)-3-bromo-4-phenyl-8-oxabicyclo[3.2.1]octa-3,6-dien-2-ol

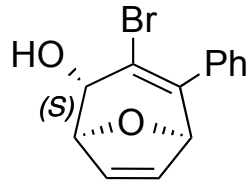

6

^{1}H NMR (500 MHz, Chloroform-*d*) δ 7.50 – 7.33 (m, 5H), 6.87 (dd, *J* = 6.0, 1.7 Hz, 1H), 6.33 (dd, *J* = 6.0, 1.9 Hz, 1H), 5.11 (dd, *J* = 19.3, 1.8 Hz, 2H), 3.91 (d, *J* = 7.9 Hz, 1H), 2.59 (d, *J* = 8.1 Hz, 1H).^{13}C NMR (126 MHz, $CDCl_3$) δ 147.84, 141.55, 136.53, 128.54, 128.49, 128.17, 127.87, 118.82, 84.46, 82.31, 70.19, 29.73. HRMS (DART) calcd for $C_{13}H_{11}BrO_2$ $[M+NH_4]^+$: 296.0286

(1R,2S,5R,6S,7R)-3-bromo-4-phenyl-8-oxabicyclo[3.2.1]oct-3-ene-2,6,7-triol

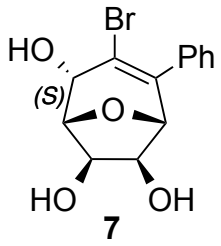

7

^{1}H NMR (500 MHz, Methanol-d_4) δ 7.49 – 7.28 (m, 5H), 4.81 (d, J = 6.1 Hz, 1H), 4.56 (d, J = 5.9 Hz, 1H), 4.50 (s, 1H), 4.32 (d, J = 5.7 Hz, 1H), 4.17 (d, J = 6.2 Hz, 1H).^{13}C NMR (126 MHz, MeOD) δ 141.62, 137.07, 128.19, 128.16, 128.02, 122.97, 86.47, 86.42, 73.33, 70.29, 69.23. HRMS (DART) calcd for $C_{13}H_{13}BrO_4$ [M-OH]$^+$: 294.9970

(1S,2S,5S,6R,7S)-3-bromo-4-phenyl-8-oxabicyclo[3.2.1]oct-3-ene-2,6,7-triol

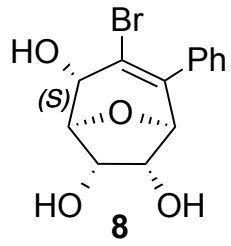

8

^{1}H NMR (500 MHz, Methanol-d_4) δ 7.48 – 7.29 (m, 5H), 4.57 (s, 1H), 4.27 (d, J = 1.3 Hz, 1H), 4.21 (d, J = 6.0 Hz, 1H), 4.11 (d, J = 6.1 Hz, 1H), 3.91 (d, J = 1.2 Hz, 1H).^{13}C NMR (126 MHz, MeOD) δ 143.61, 138.28, 129.47, 129.41, 129.36, 120.84, 89.52, 86.73, 73.80, 73.30, 72.94. HRMS (DART) calcd for $C_{13}H_{13}BrO_4$ [M+NH_4]$^+$: 330.0341

(1R,2R,5S)-3-bromo-4-phenyl-8-oxabicyclo[3.2.1]octa-3,6-dien-2-ol

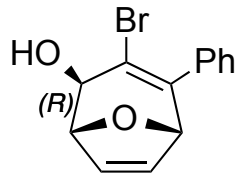

9

^{1}H NMR (500 MHz, Chloroform-*d*) δ 7.49 – 7.33 (m, 5H), 6.88 (dd, *J* = 5.9, 1.8 Hz, 1H), 6.33 (dd, *J* = 6.0, 2.0 Hz, 1H), 5.13 (d, *J* = 2.0 Hz, 1H), 5.09 (d, *J* = 1.8 Hz, 1H), 3.91 (d, *J* = 8.1 Hz, 1H), 2.56 (s, 1H).^{13}C NMR (126 MHz, $CDCl_3$) δ 147.86, 141.57, 136.53, 128.54, 128.50, 128.17, 127.86, 118.82, 84.45, 82.32, 70.19. HRMS (DART) calcd for $C_{13}H_{11}BrO_2$ $[M+H]^+$: 296.0286

(1S,2R,5R)-3-bromo-4-phenyl-8-oxabicyclo[3.2.1]octa-3,6-dien-2-ol

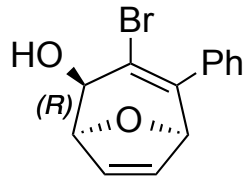

10

^{1}H NMR (500 MHz, Chloroform-*d*) δ 7.56 – 7.33 (m, 5H), 6.90 (dd, *J* = 6.0, 1.7 Hz, 1H), 6.34 (dd, *J* = 5.9, 1.8 Hz, 1H), 5.33 (dd, *J* = 6.1, 1.8 Hz, 1H), 4.98 (d, *J* = 1.7 Hz, 1H), 4.65 (t, *J* = 5.2 Hz, 1H), 2.26 (d, *J* = 4.7 Hz, 1H).^{13}C NMR (126 MHz, $CDCl_3$) δ 146.52, 140.80, 136.52, 129.31, 128.51, 128.38, 127.84, 121.62, 83.13, 81.80, 67.93. HRMS (DART) calcd for $C_{13}H_{11}BrO_2$ $[M-OH]^+$: 260.9915

(1R,2R,5R,6S,7R)-3-bromo-4-phenyl-8-oxabicyclo[3.2.1]oct-3-ene-2,6,7-triol

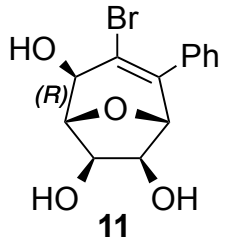

11

^{1}H NMR (500 MHz, Methanol-d_4) δ 7.47 – 7.30 (m, 5H), 4.61 (d, J = 1.0 Hz, 1H), 4.31 (q, J = 1.3 Hz, 1H), 4.23 (d, J = 6.0 Hz, 1H), 4.13 (d, J = 6.0 Hz, 1H), 3.93 (d, J = 1.3 Hz, 1H).^{13}C NMR (126 MHz, MeOD) δ 143.61, 138.28, 129.47, 129.41, 129.36, 120.84, 89.52, 86.73, 73.80, 73.30, 72.94. HRMS (DART) calcd for $C_{13}H_{13}BrO_4$ [M-OH]$^{+}$: 294.9970

(1S,2R,5S,6R,7S)-3-bromo-4-phenyl-8-oxabicyclo[3.2.1]oct-3-ene-2,6,7-triol

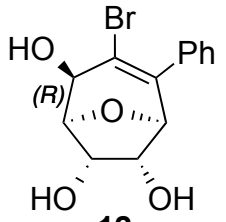

12

^{1}H NMR (500 MHz, Methanol-d_4) δ 7.47 – 7.29 (m, 5H), 4.81 (d, J = 6.1 Hz, 1H), 4.61 – 4.53 (m, 1H), 4.50 (s, 1H), 4.32 (d, J = 5.8 Hz, 1H), 4.17 (d, J = 6.2 Hz, 1H). ^{13}C NMR (126 MHz, MeOD) δ 141.62, 137.07, 128.19, 128.16, 128.02, 122.96, 86.47, 86.42, 73.33, 70.29, 69.23. HRMS (DART) calcd for $C_{13}H_{13}BrO_4$ [M-OH]$^{+}$: 294.9970

3,4-dibromo-8-oxabicyclo[3.2.1]octa-3,6-dien-2-yl3-{[(tertbutoxy)carbonyl]amino}propanoate

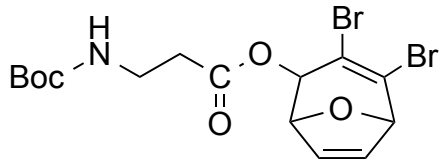

13

^{1}H NMR (500 MHz, Methanol-d_4) δ 6.96 (dd, J = 5.9, 1.9 Hz, 1H), 6.36 – 6.26 (m, 1H), 5.78 (d, J = 6.0 Hz, 1H), 5.26 (dd, J = 6.0, 2.0 Hz, 1H), 4.95 (d, J = 1.8 Hz, 1H), 3.37 – 3.29 (m, 2H), 2.59 (t, J = 6.5 Hz, 2H), 1.45 (s, 9H).^{13}C NMR (126 MHz, MeOD) δ 170.79, 138.74, 131.08, 129.90, 118.75, 84.05, 83.56, 82.45, 79.58, 79.41, 78.84, 69.55, 35.96, 33.99, 27.39. HRMS (DART) calcd for $C_{15}H_{19}Br_2NO_5$ $[M+H]^+$: 453.9689

3,4-dibromo-6,7-dihydroxy-8-oxabicyclo[3.2.1]oct-3-en-2-yl 3-{[(tert-butoxy)carbonyl]amino}propanoate

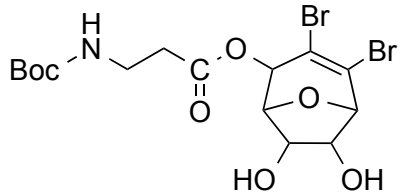

14

^{1}H NMR (500 MHz, Methanol-d_4) δ 5.76 (d, J = 5.5 Hz, 1H), 4.60 (d, J = 6.4 Hz, 1H), 4.50 (s, 1H), 4.43 – 4.35 (m, 1H), 4.25 (d, J = 6.2 Hz, 1H), 3.41 – 3.33 (m, 2H), 2.63 (t, J = 6.8 Hz, 2H), 1.43 (s, 10H).^{13}C NMR (126 MHz, MeOD) δ 171.97, 127.92, 122.10, 89.09, 84.89, 74.65, 72.44, 72.23, 37.35, 35.53, 28.83. HRMS (DART) calcd for $C_{15}H_{21}Br_2NO_5$ $[M+H]^+$: 487.9744

3,4-dibromo-6,7-dihydroxy-8-oxabicyclo[3.2.1]oct-3-en-2-yl 3-aminopropanoate

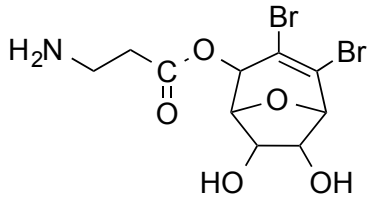

15

^{1}H NMR (500 MHz, Methanol-d_4) δ 5.84 (d, J = 5.5 Hz, 1H), 5.76 (d, J = 5.7 Hz, 1H), 4.58 (q, J = 7.6 Hz, 3H), 4.55 (s, 2H), 4.45 (t, J = 6.4 Hz, 2H), 4.36 (s, 3H), 4.29 (d, J = 6.2 Hz, 1H), 3.29 (t, J = 5.1 Hz, 5H), 2.91 (t, J = 6.3 Hz, 7H). HRMS (DART) calcd for $C_{10}H_{13}Br_2NO_5$ $[M+H]^+$: 387.9219

3,4-dibromo-8-oxabicyclo[3.2.1]octa-3,6-dien-2-yl 2-({[(9H-fluoren-9-yl)methoxy]carbonyl}amino)acetate

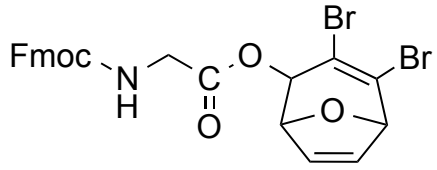

16

^{1}H NMR (500 MHz, Chloroform-d) δ 7.82 (d, J = 7.5 Hz, 2H), 7.64 (t, J = 6.2 Hz, 2H), 7.46 (t, J = 7.5 Hz, 2H), 7.37 (td, J = 7.4, 1.1 Hz, 2H), 6.90 (d, J = 5.9 Hz, 1H), 6.23 (d, J = 5.9 Hz, 1H), 5.86 (d, J = 5.9 Hz, 1H), 5.40 – 5.26 (m, 2H), 4.96 (d, J = 1.7 Hz, 1H), 4.48 (d, J = 7.2 Hz, 2H), 4.30 (t, J = 7.0 Hz, 1H), 4.09 (qd, J = 18.4, 5.8 Hz, 2H).^{13}C NMR (126 MHz, $CDCl_3$) δ 169.23, 156.31, 143.72, 141.36, 139.41, 131.72, 129.70, 127.81, 127.15, 125.08, 120.07, 118.39, 84.18, 79.54, 70.54, 67.40, 47.11, 42.67. HRMS (DART) calcd for $C_{24}H_{19}Br_2NO_5$ $[M+H]^+$: 561.9690

3,4-dibromo-6,7-dihydroxy-8-oxabicyclo[3.2.1]oct-3-en-2-yl 2-({[(9H-fluoren-9-yl)methoxy]carbonyl}amino)acetate

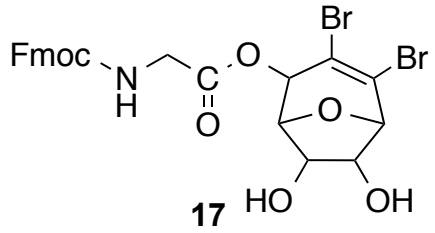

17

To a flask compound **16** (0.107mmol, 30mg) and Fmoc-Gly-OH (0.107mmol, 31.8) were added in solution (Acetonitrile, 2mL). The suspension was warmed at 35ºC and stirred until changing into clear. Then follow the general procedure for esterification. ^{1}H NMR (500 MHz, Chloroform-*d*) δ 7.79 (d, *J* = 7.5 Hz, 2H), 7.59 (t, *J* = 6.5 Hz, 2H), 7.43 (t, *J* = 7.5 Hz, 2H), 7.38 – 7.30 (m, 2H), 5.76 (dd, *J* = 16.5, 5.5 Hz, 1H), 5.42 (s, 1H), 4.62 (t, *J* = 5.5 Hz, 1H), 4.60 (s, 1H), 4.52 (d, *J* = 5.6 Hz, 1H), 4.51 – 4.39 (m, 3H), 4.25 (dq, *J* = 15.4, 8.4, 7.3 Hz, 2H), 4.09 – 3.96 (m, 2H).

APPENDIX SELECTED SPECTRA

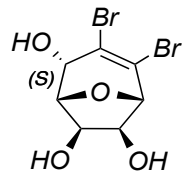
Br
HO
(S)
Br
O
HO
OH

1

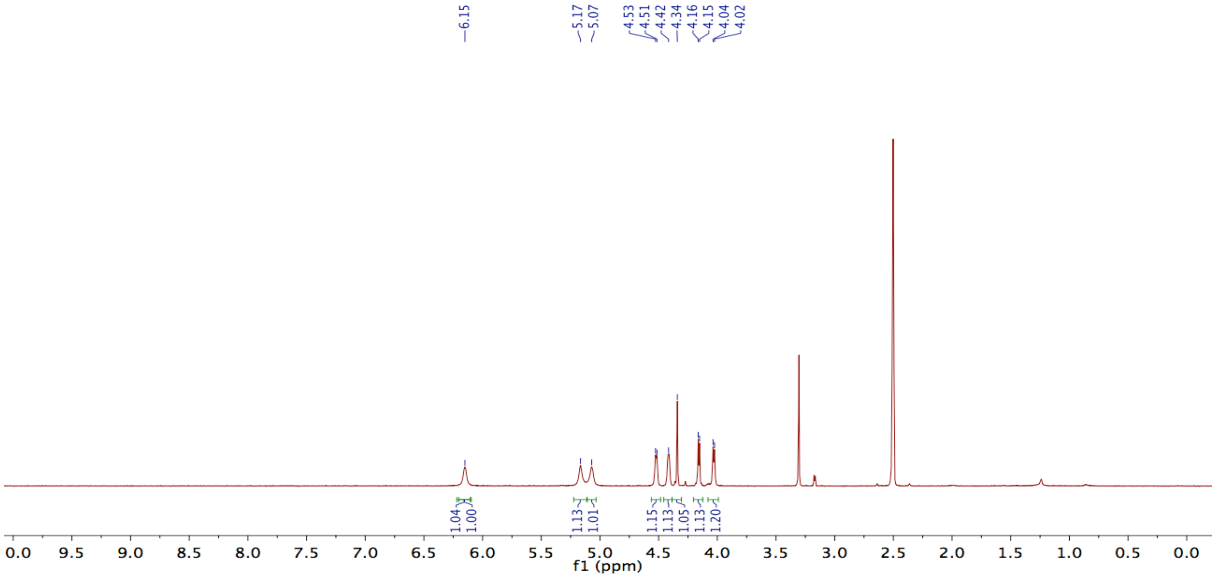
6.15
5.17
5.07
4.53
4.51
4.42
4.34
4.16
4.15
4.04
4.02
1.04
1.00
1.13
1.01
1.15
1.13
1.05
1.13
1.20
f1 (ppm)

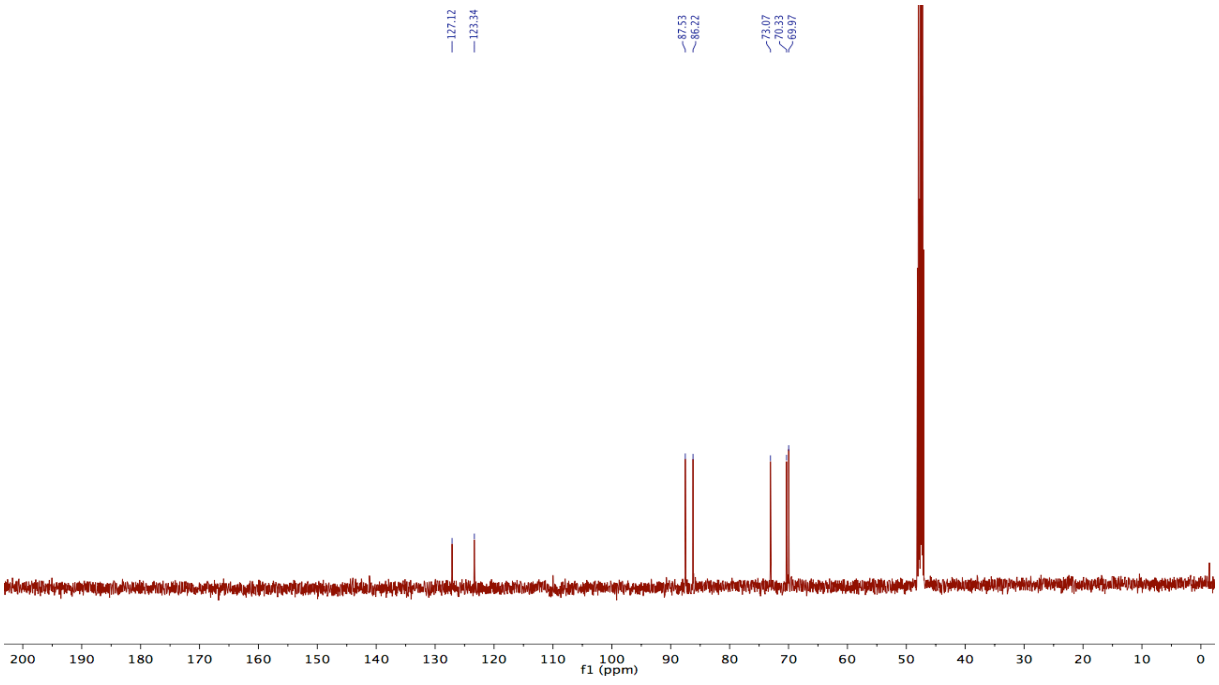
127.12
123.34
87.53
86.22
73.07
70.33
69.97
f1 (ppm)

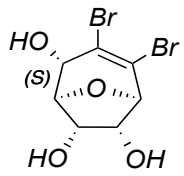
Br
HO
Br
(S)
O
HO
OH

2

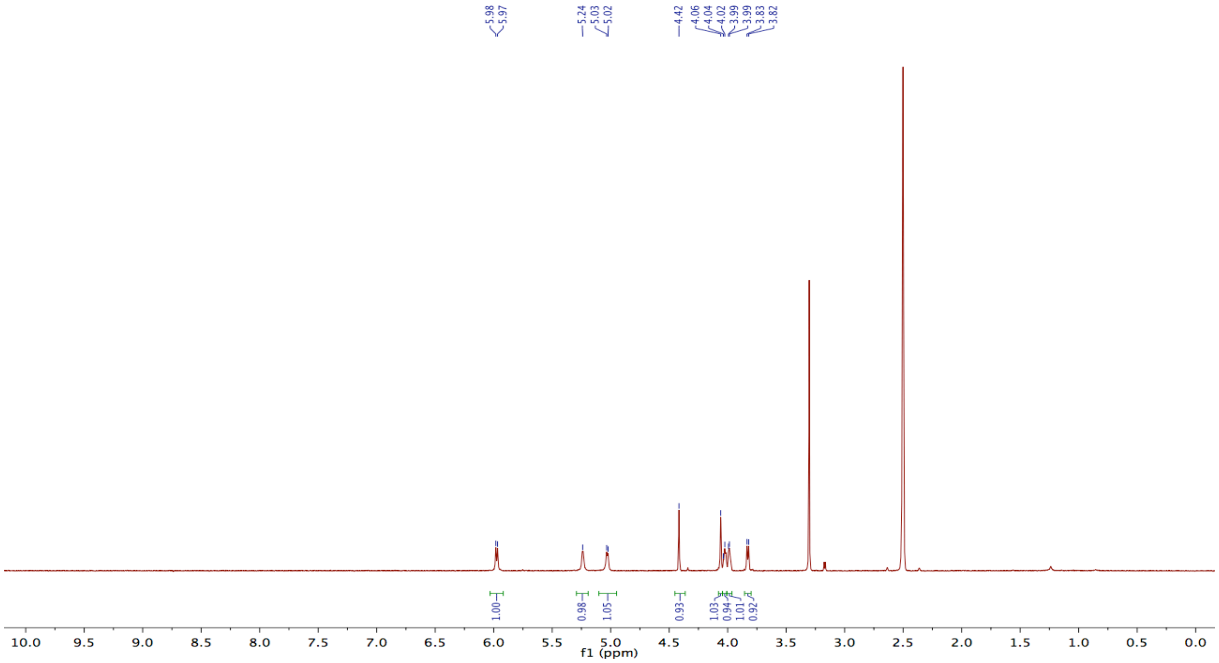
5.98
5.97
5.24
5.03
5.02
4.42
4.06
4.04
4.02
3.99
3.99
3.83
3.82
1.00
0.98
1.05
0.93
1.03
0.94
1.01
0.92
f1 (ppm)

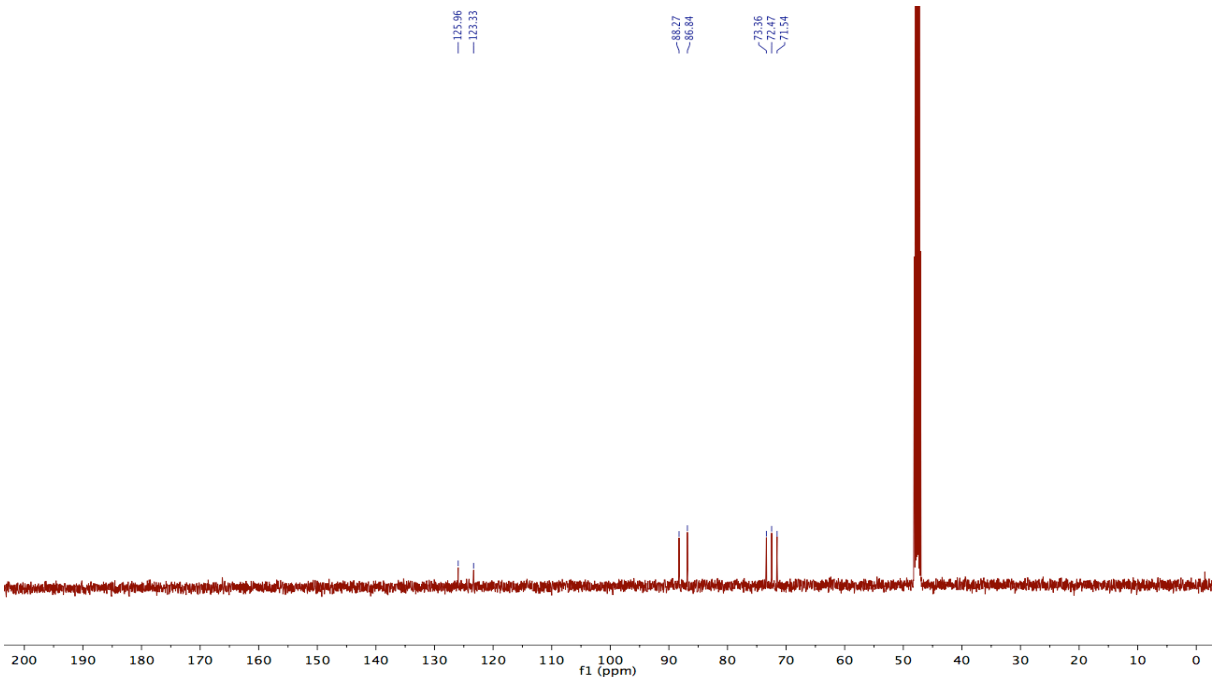
125.96
123.33
88.27
86.84
73.36
72.47
71.54
f1 (ppm)

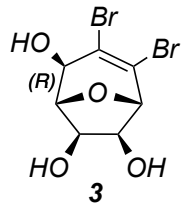
Br
HO
Br
(R)
O
HO
OH

3

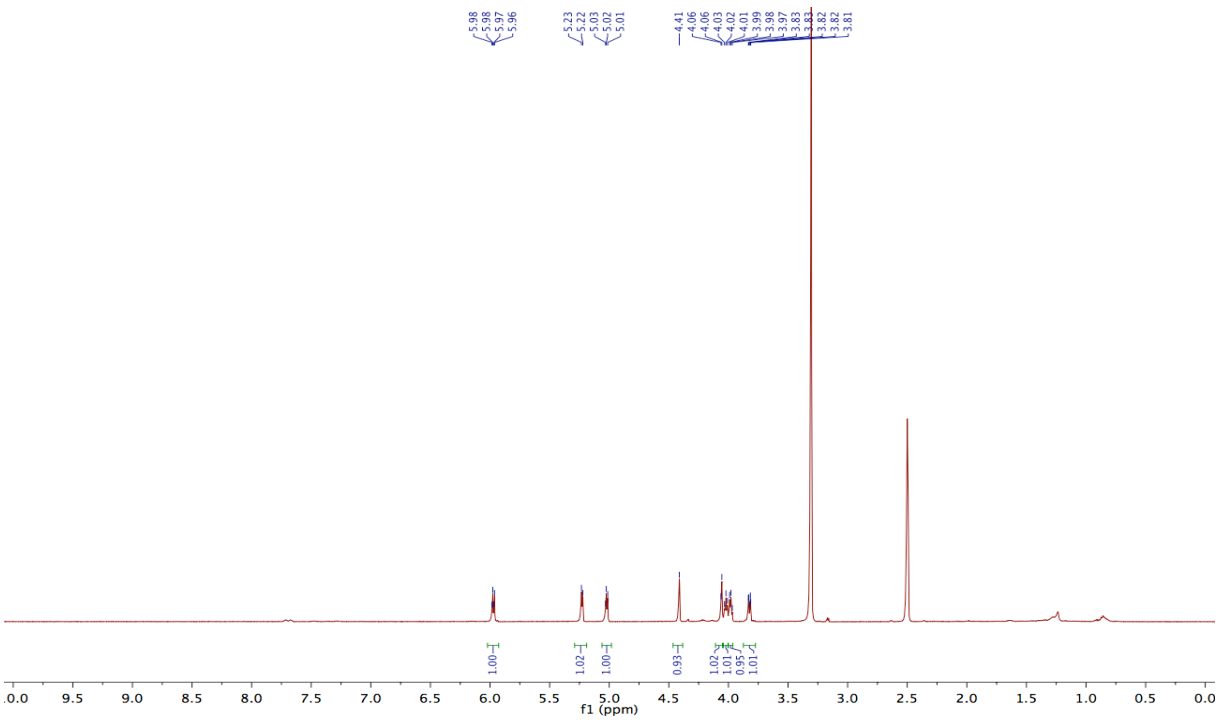
5.98
5.98
5.97
5.96
5.23
5.22
5.03
5.02
5.01
4.41
4.06
4.06
4.03
4.02
4.01
3.99
3.98
3.97
3.83
3.83
3.82
3.82
3.81
1.00
1.02
1.00
0.93
1.02
1.01
0.95
1.01
f1 (ppm)

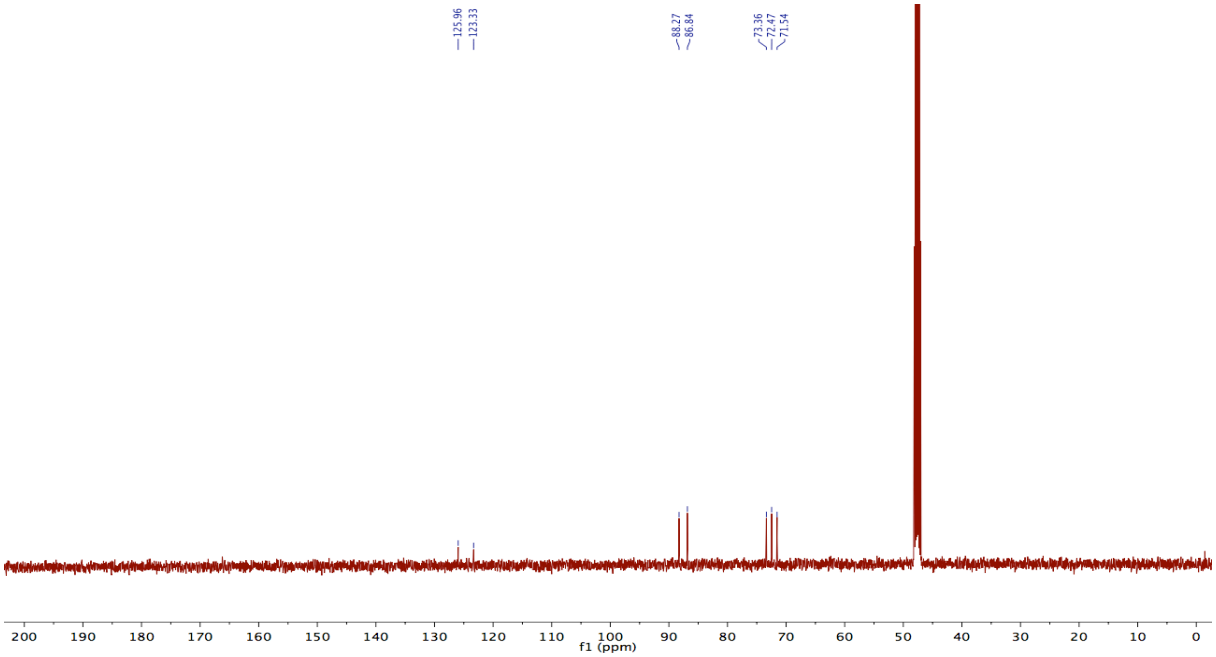
125.96
123.33
88.27
86.84
73.36
72.47
71.54
f1 (ppm)

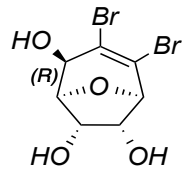
Br
HO
Br
(R)
O
HO
OH

4

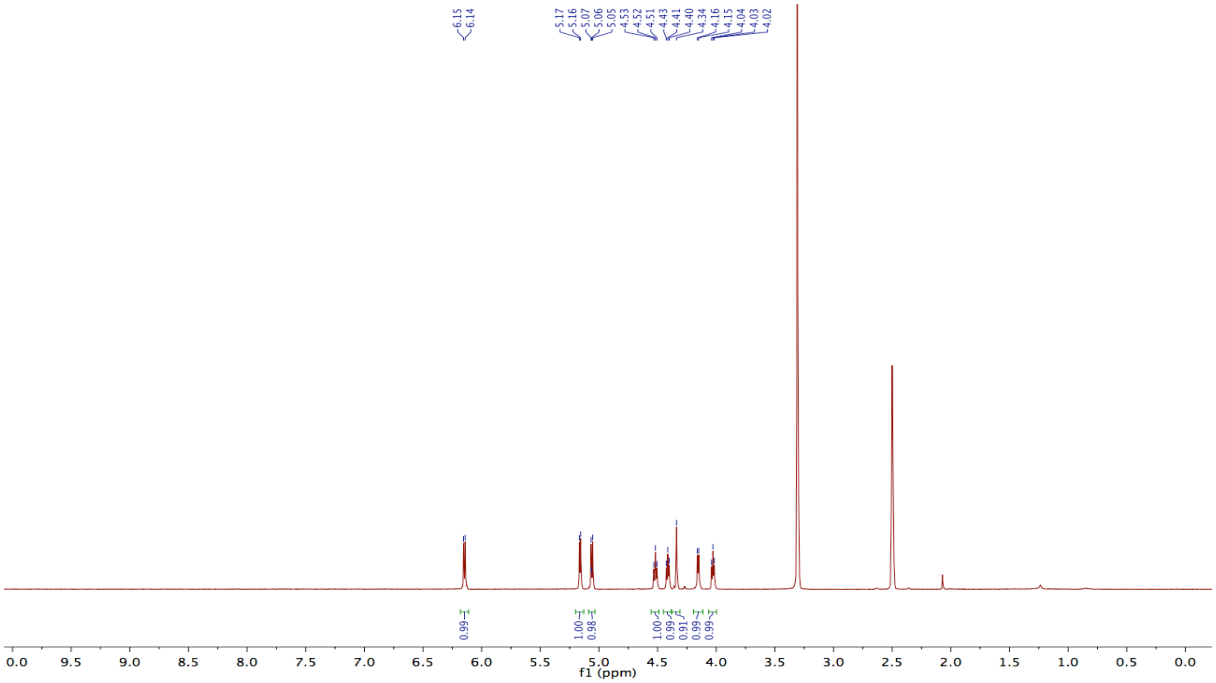
6.15
6.14
5.17
5.16
5.07
5.06
5.05
4.53
4.52
4.51
4.43
4.41
4.40
4.34
4.16
4.15
4.04
4.03
4.02
0.99
1.00
0.98
1.00
0.99
0.91
0.99
0.99
f1 (ppm)

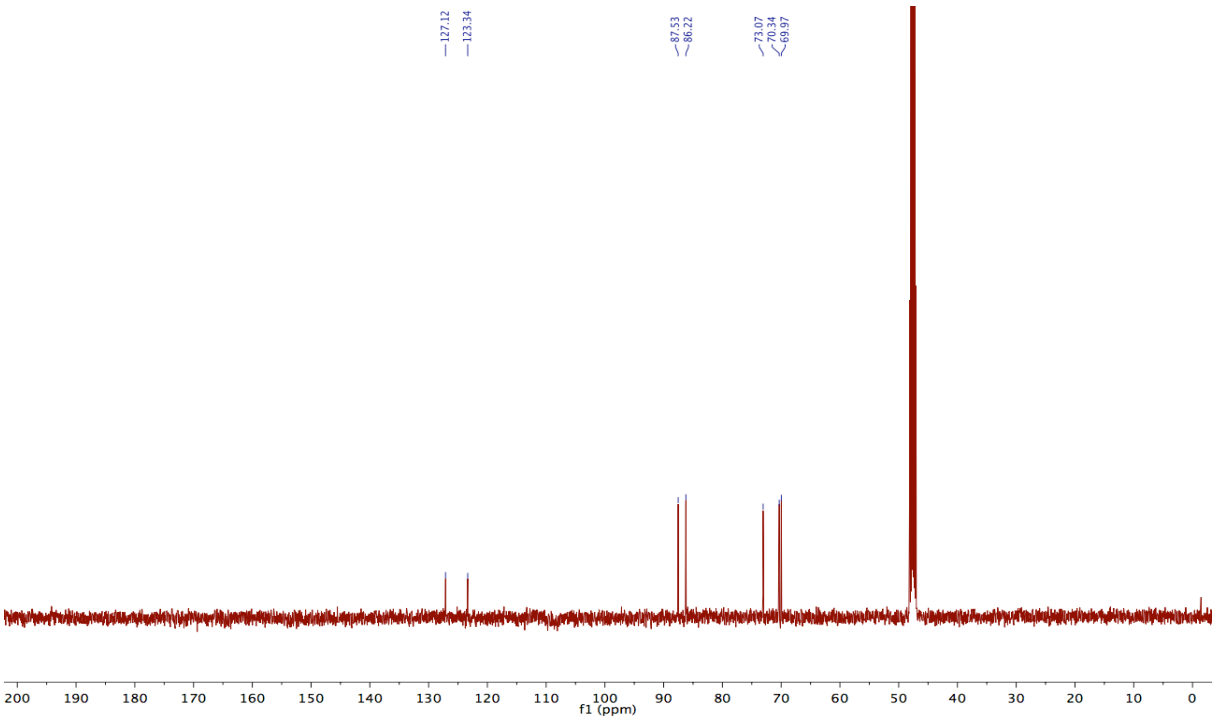
127.12
123.34
87.53
86.22
73.07
70.34
69.97
f1 (ppm)

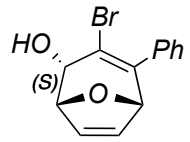
Br
HO
Ph
(S)
O

5

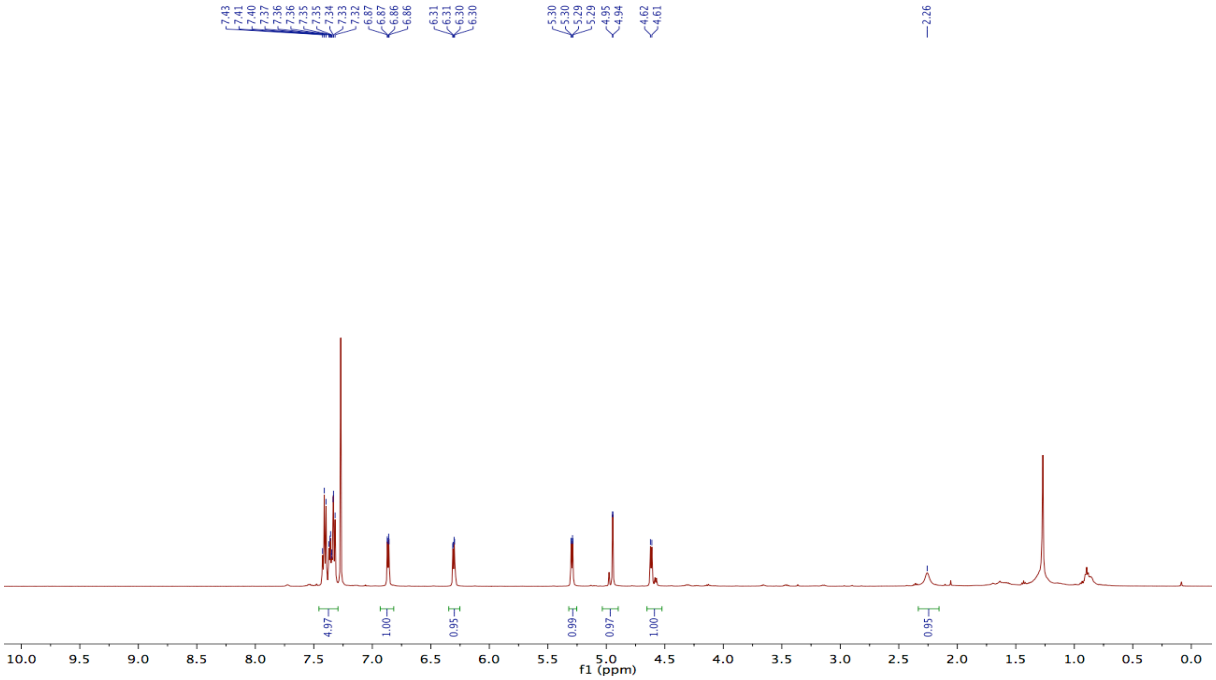
7.43
7.41
7.40
7.37
7.36
7.36
7.35
7.35
7.34
7.33
7.32
6.87
6.87
6.86
6.86
6.31
6.31
6.30
6.30
5.30
5.30
5.29
5.29
4.95
4.94
4.62
4.61
2.26
4.97
1.00
0.95
0.99
0.97
1.00
0.95
f1 (ppm)

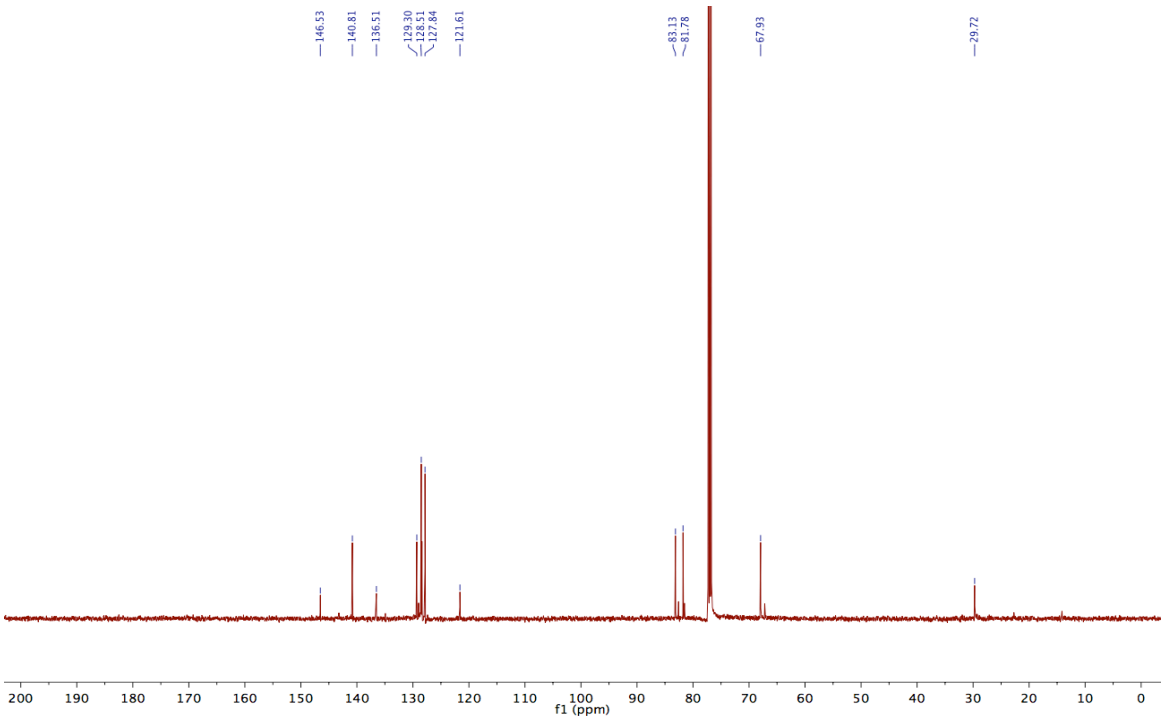
146.53
140.81
136.51
129.30
128.51
127.84
121.61
83.13
81.78
67.93
29.72
f1 (ppm)

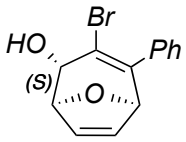
Br
HO
Ph
(S)
O

6


7.47
7.46
7.45
7.43
7.42
7.41
7.40
7.37
7.36
7.35
6.88
6.87
6.34
6.33
6.32
5.13
5.12
5.09
3.92
3.90
2.60
2.58

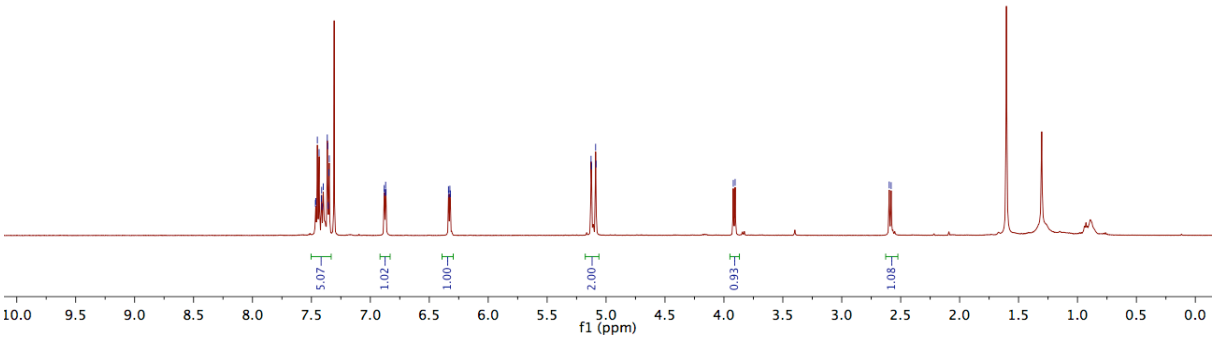
5.07
1.02
1.00
2.00
0.93
1.08
f1 (ppm)

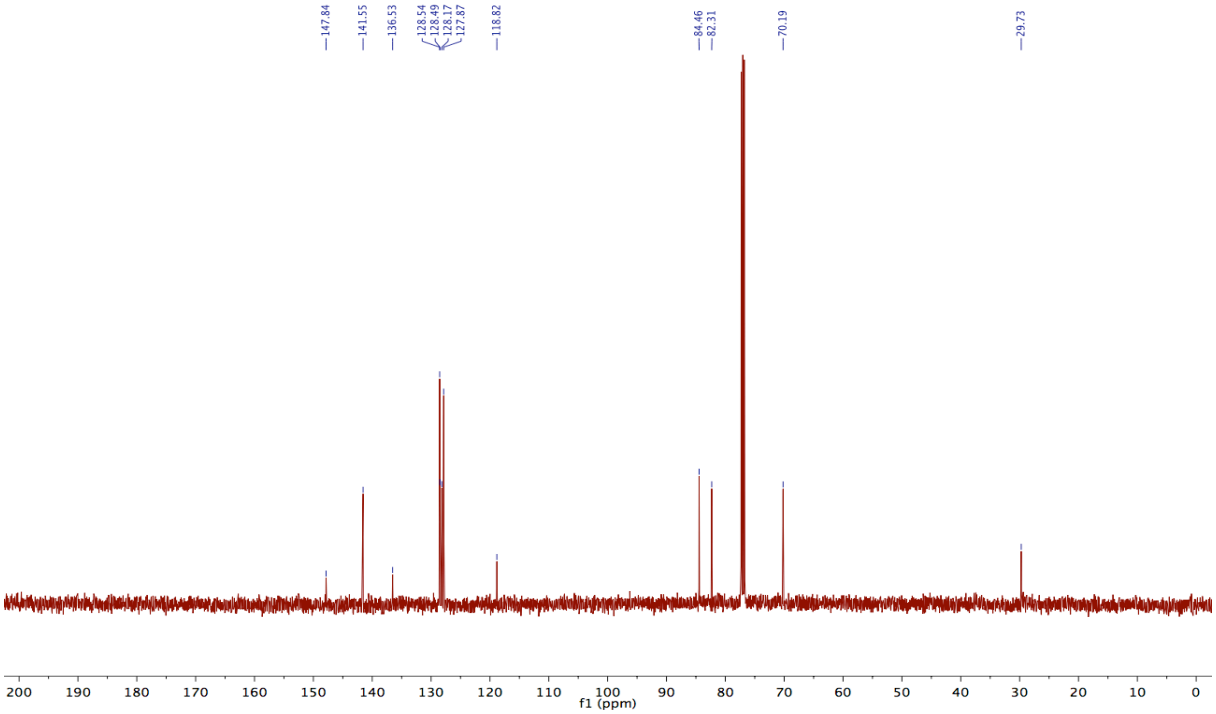
147.84
141.55
136.53
128.54
128.49
128.17
127.87
118.82
84.46
82.31
70.19
29.73
f1 (ppm)

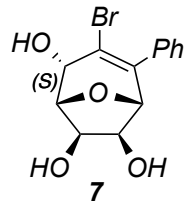
Br
HO
Ph
(S)
O
HO
OH

7

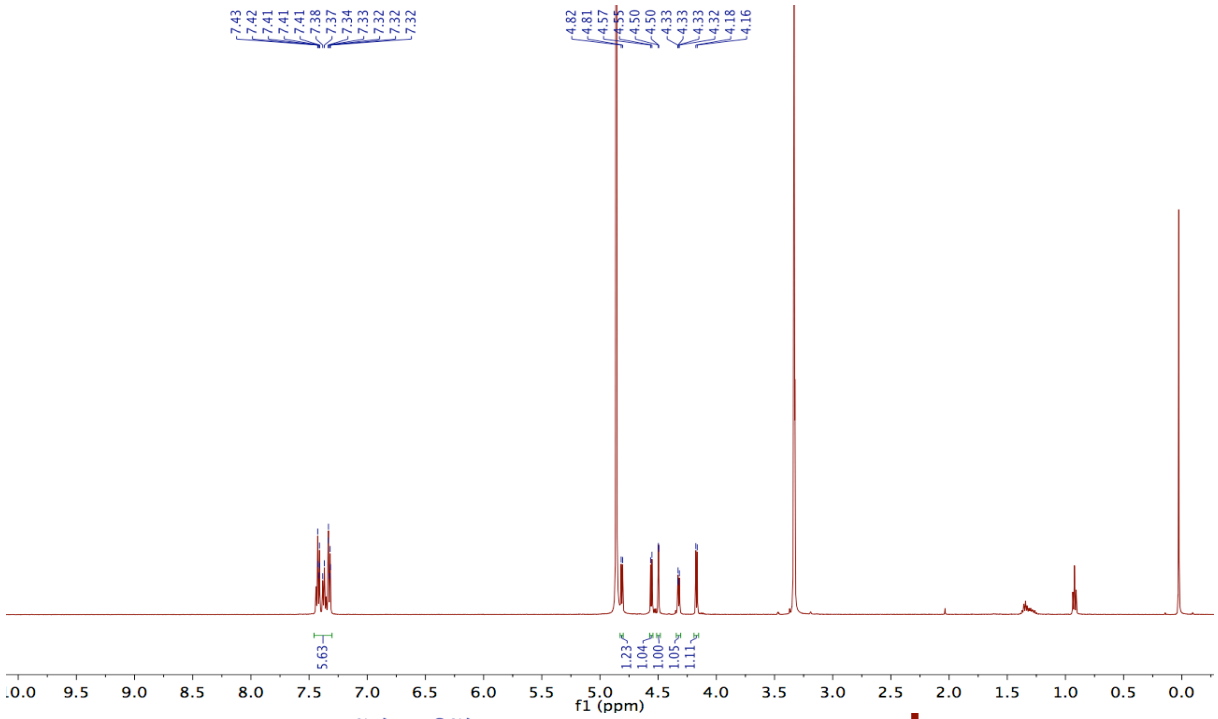
7.43
7.42
7.41
7.41
7.41
7.38
7.37
7.34
7.33
7.32
7.32
7.32
4.82
4.81
4.57
4.55
4.50
4.50
4.33
4.33
4.33
4.32
4.18
4.16
5.63
1.23
1.04
1.00
1.05
1.11
f1 (ppm)

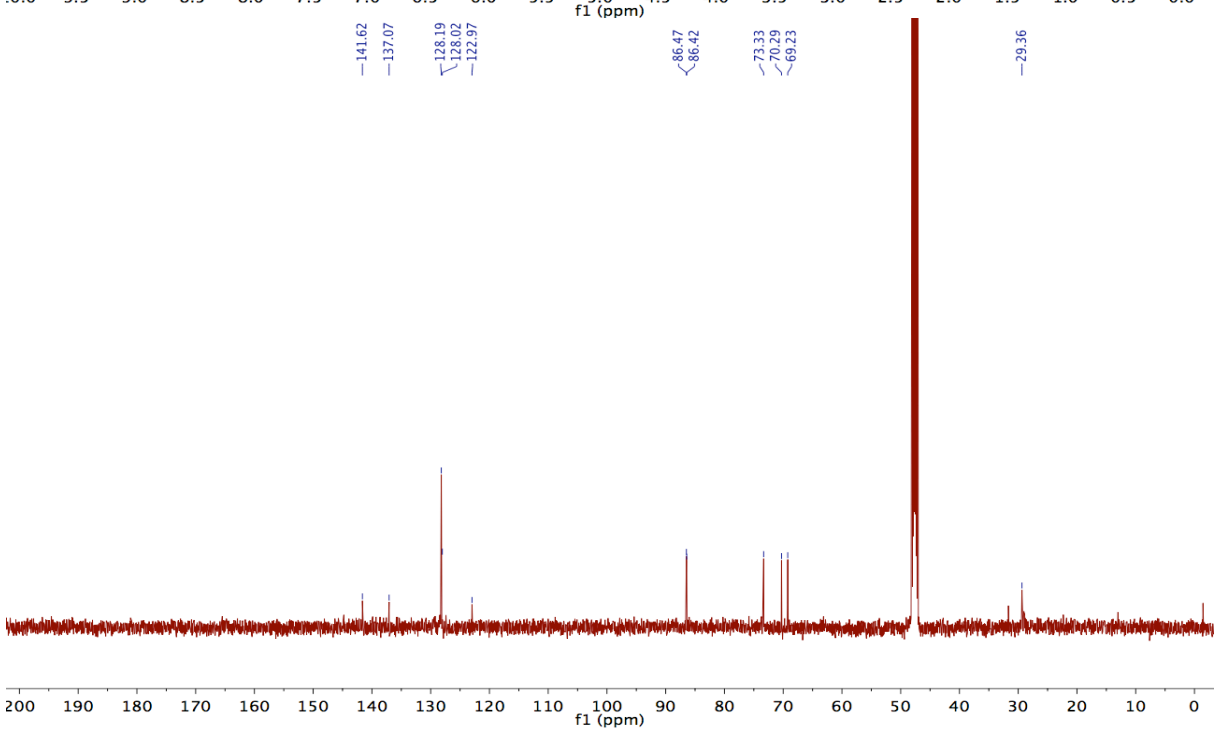
141.62
137.07
128.19
128.02
122.97
86.47
86.42
73.33
70.29
69.23
29.36
f1 (ppm)

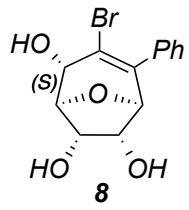
Br
HO
Ph
(S)
O
HO
OH

8

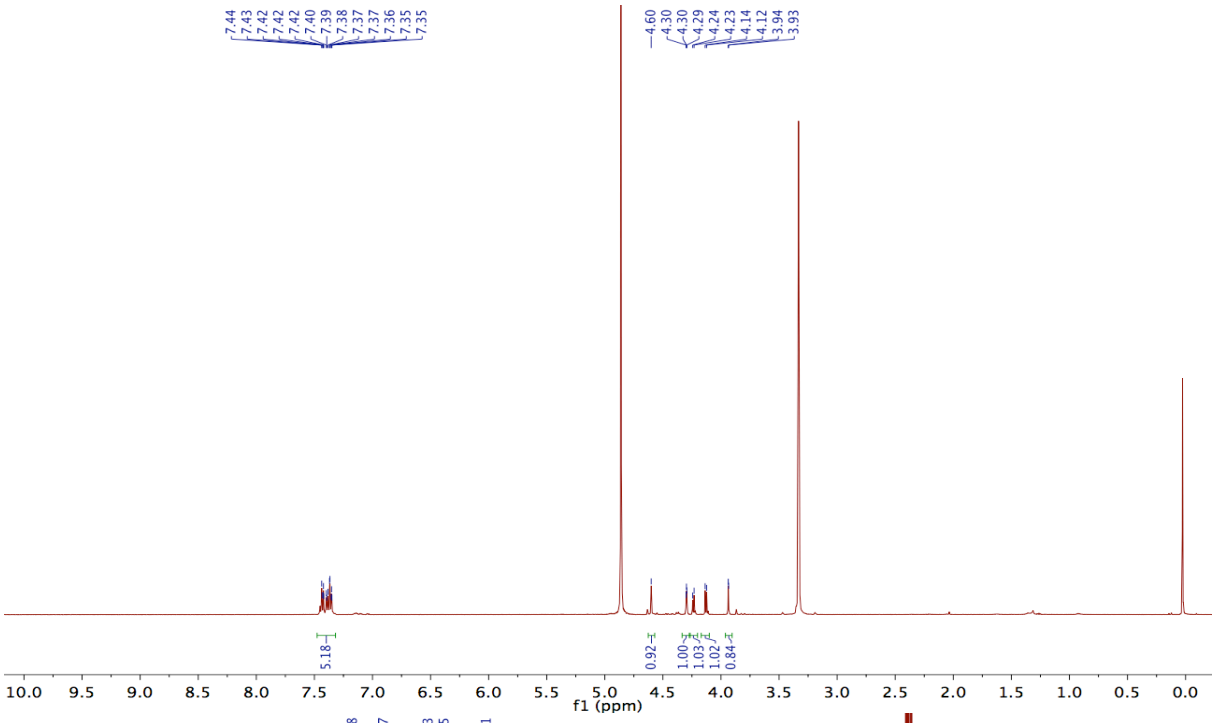
7.44
7.43
7.42
7.42
7.42
7.40
7.39
7.38
7.37
7.37
7.36
7.35
7.35
4.60
4.30
4.30
4.29
4.24
4.23
4.14
4.12
3.94
3.93
5.18
0.92
1.00
1.03
1.02
0.84
f1 (ppm)

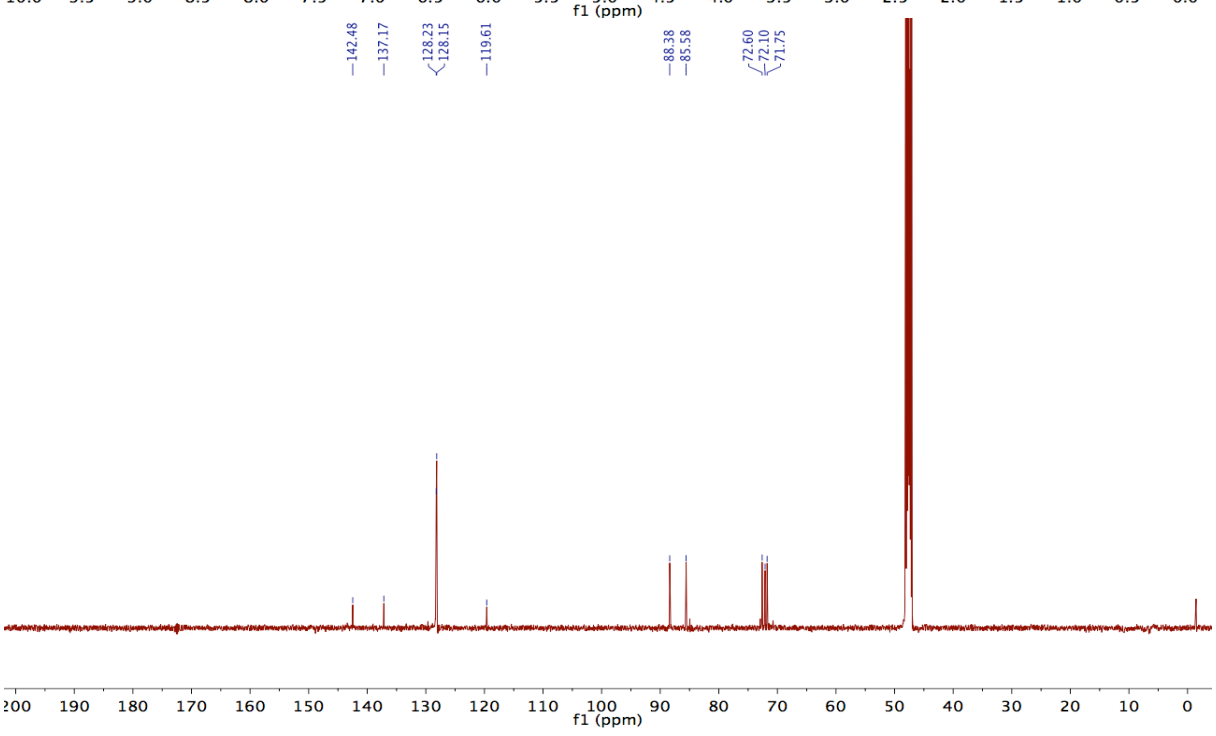
142.48
137.17
128.23
128.15
119.61
88.38
85.58
72.60
72.10
71.75
f1 (ppm)

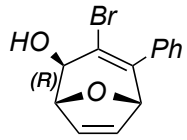
Br
HO
Ph
(R)
O

9

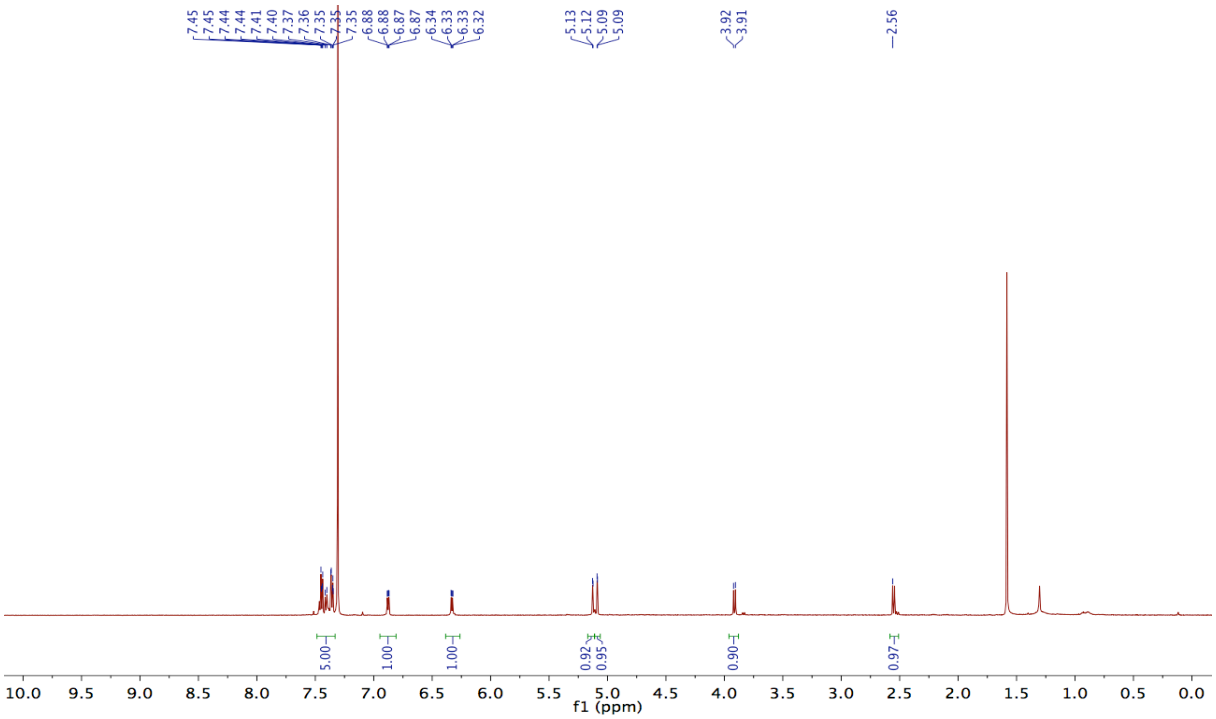
7.45
7.45
7.44
7.44
7.41
7.40
7.37
7.36
7.35
7.35
7.35
6.88
6.88
6.87
6.87
6.34
6.33
6.33
6.32
5.13
5.12
5.09
5.09
3.92
3.91
2.56
5.00
1.00
1.00
0.92
0.95
0.90
0.97
10.0 9.5 9.0 8.5 8.0 7.5 7.0 6.5 6.0 5.5 5.0 4.5 4.0 3.5 3.0 2.5 2.0 1.5 1.0 0.5 0.0
f1 (ppm)

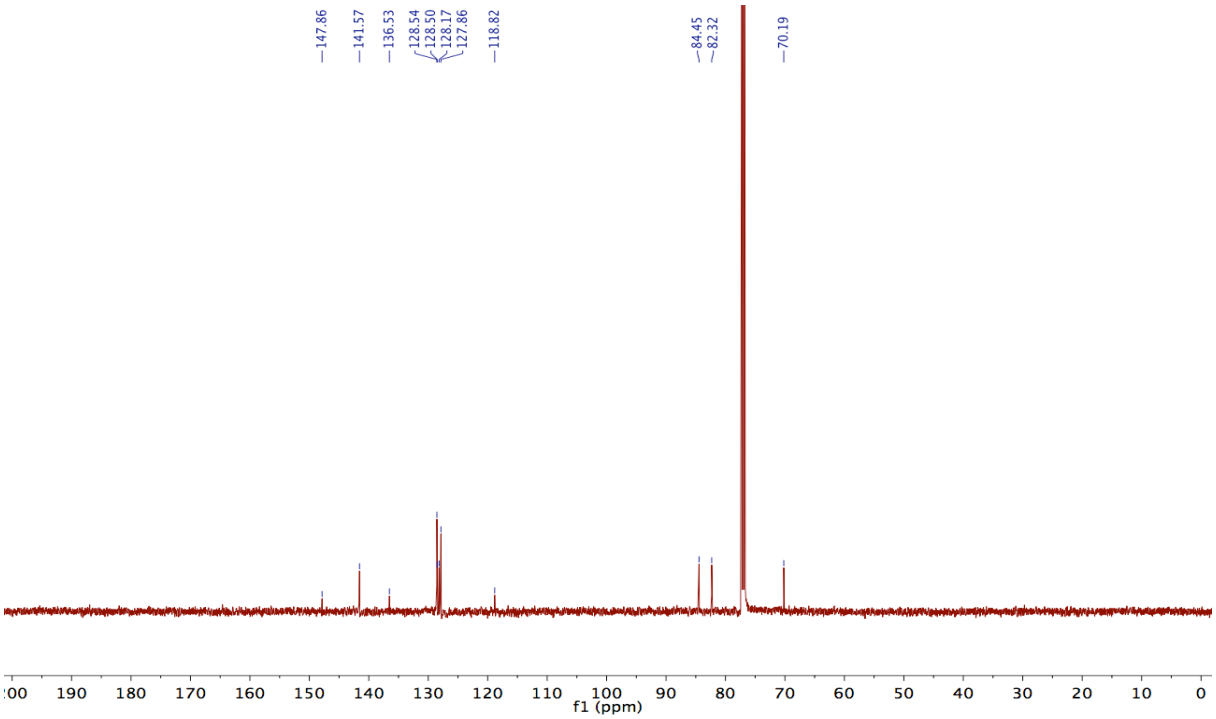
147.86
141.57
136.53
128.54
128.50
128.17
127.86
118.82
84.45
82.32
70.19
190 180 170 160 150 140 130 120 110 100 90 80 70 60 50 40 30 20 10 0
f1 (ppm)

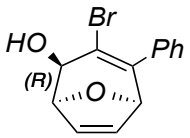
Br
HO
Ph
(R)
O

10

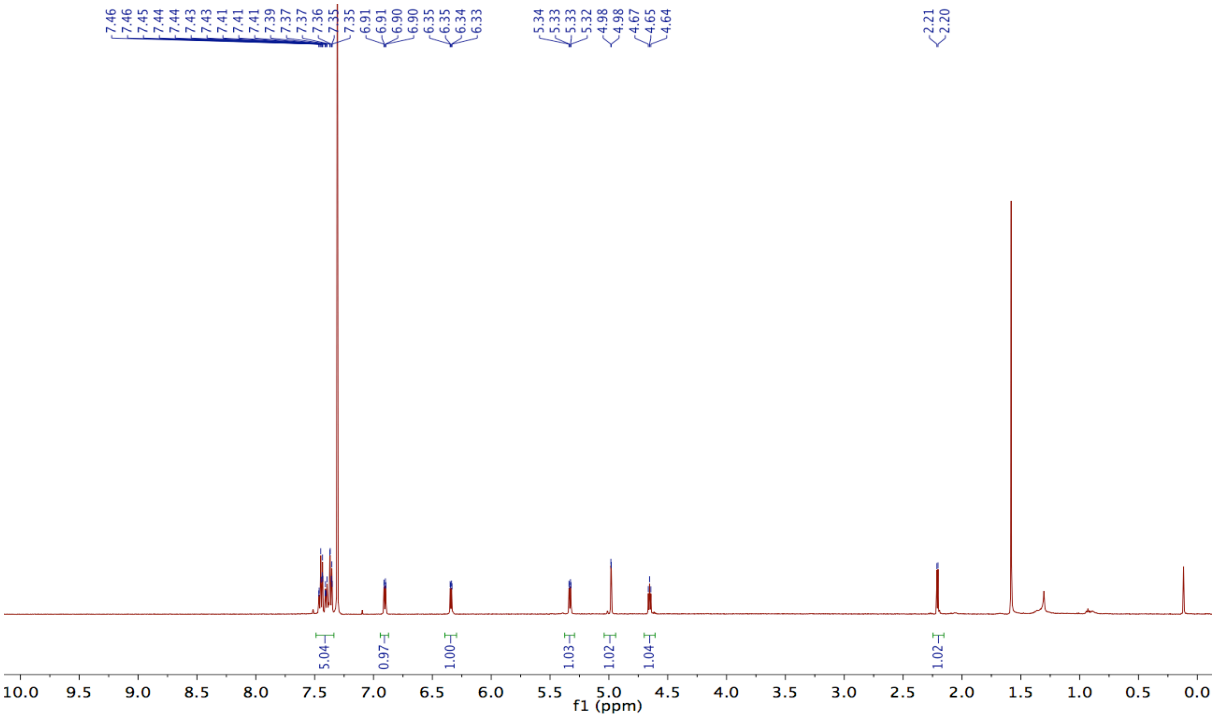
7.46
7.46
7.45
7.44
7.44
7.43
7.43
7.41
7.41
7.41
7.39
7.37
7.37
7.36
7.35
7.35
6.91
6.91
6.90
6.90
6.35
6.35
6.34
6.33
5.34
5.33
5.33
5.32
4.98
4.98
4.67
4.65
4.64
2.21
2.20
5.04
0.97
1.00
1.03
1.02
1.04
1.02
10.0 9.5 9.0 8.5 8.0 7.5 7.0 6.5 6.0 5.5 5.0 4.5 4.0 3.5 3.0 2.5 2.0 1.5 1.0 0.5 0.0
f1 (ppm)

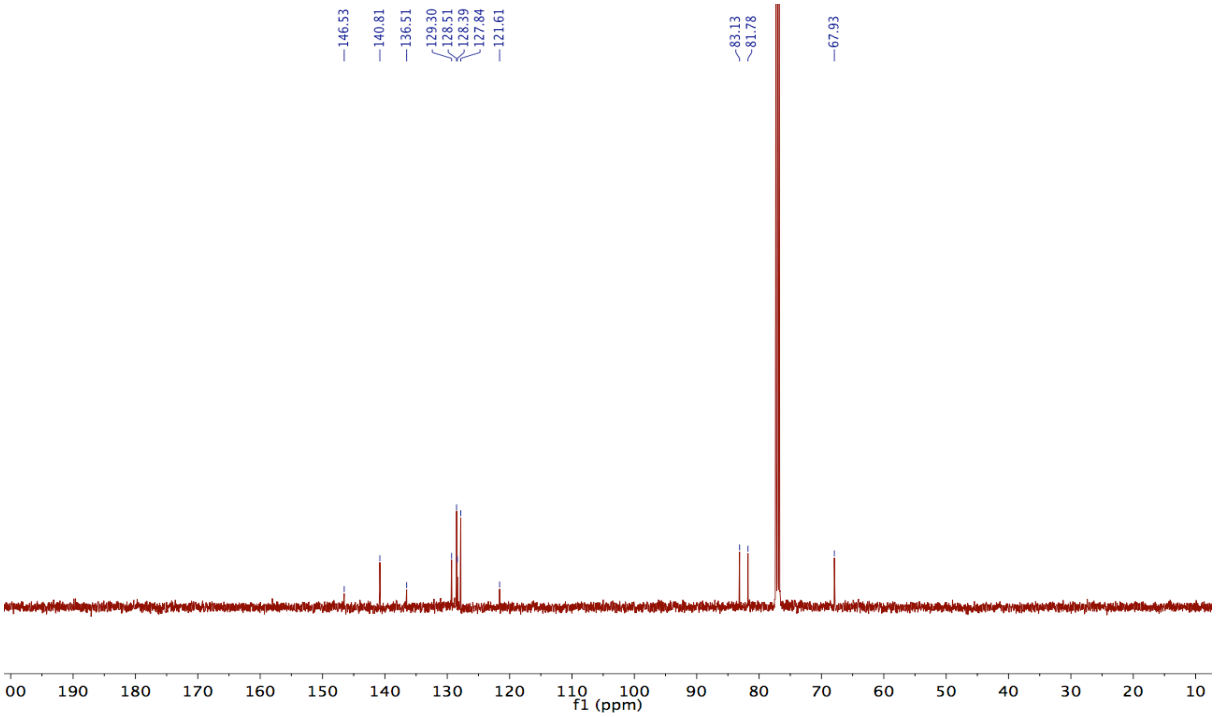
146.53
140.81
136.51
129.30
128.51
128.39
127.84
121.61
83.13
81.78
67.93
00 190 180 170 160 150 140 130 120 110 100 90 80 70 60 50 40 30 20 10
f1 (ppm)

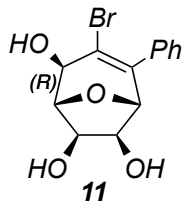
Br
HO
Ph
(R)
O
HO
OH

11

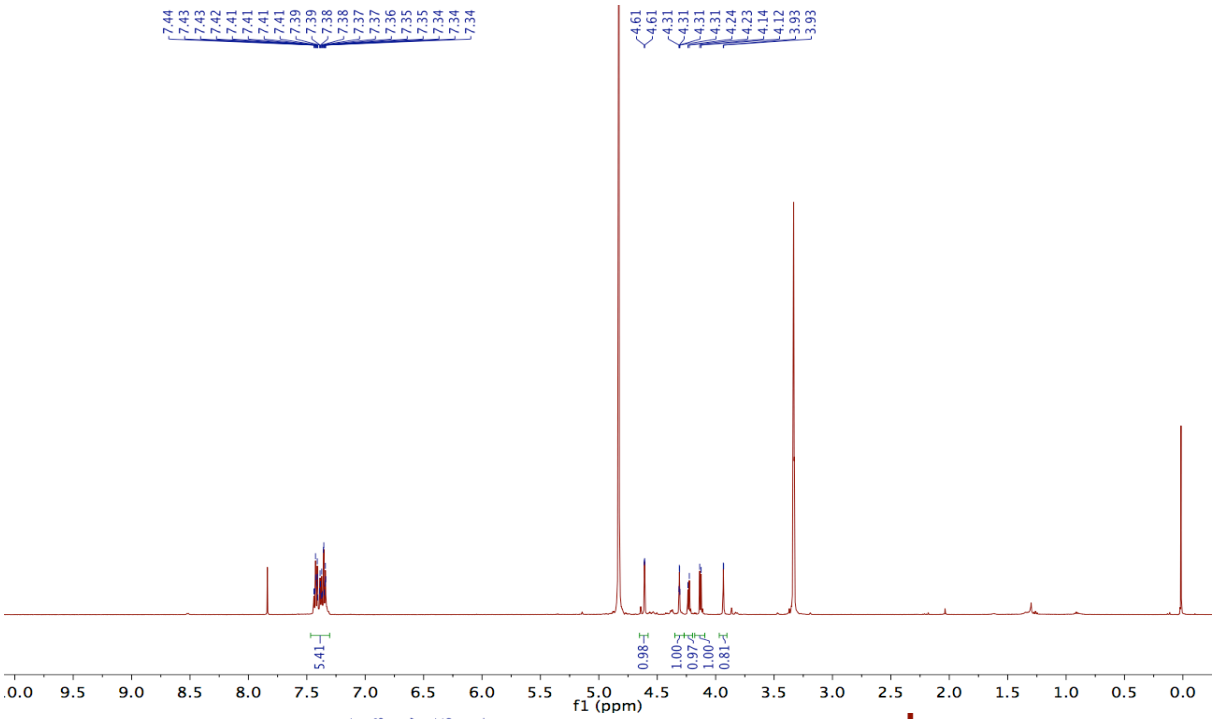
7.44
7.43
7.43
7.42
7.41
7.41
7.41
7.41
7.39
7.39
7.38
7.38
7.37
7.37
7.36
7.35
7.35
7.34
7.34
7.34
4.61
4.61
4.31
4.31
4.31
4.31
4.24
4.23
4.14
4.12
3.93
3.93
5.41
0.98
1.00
0.97
1.00
0.81
f1 (ppm)

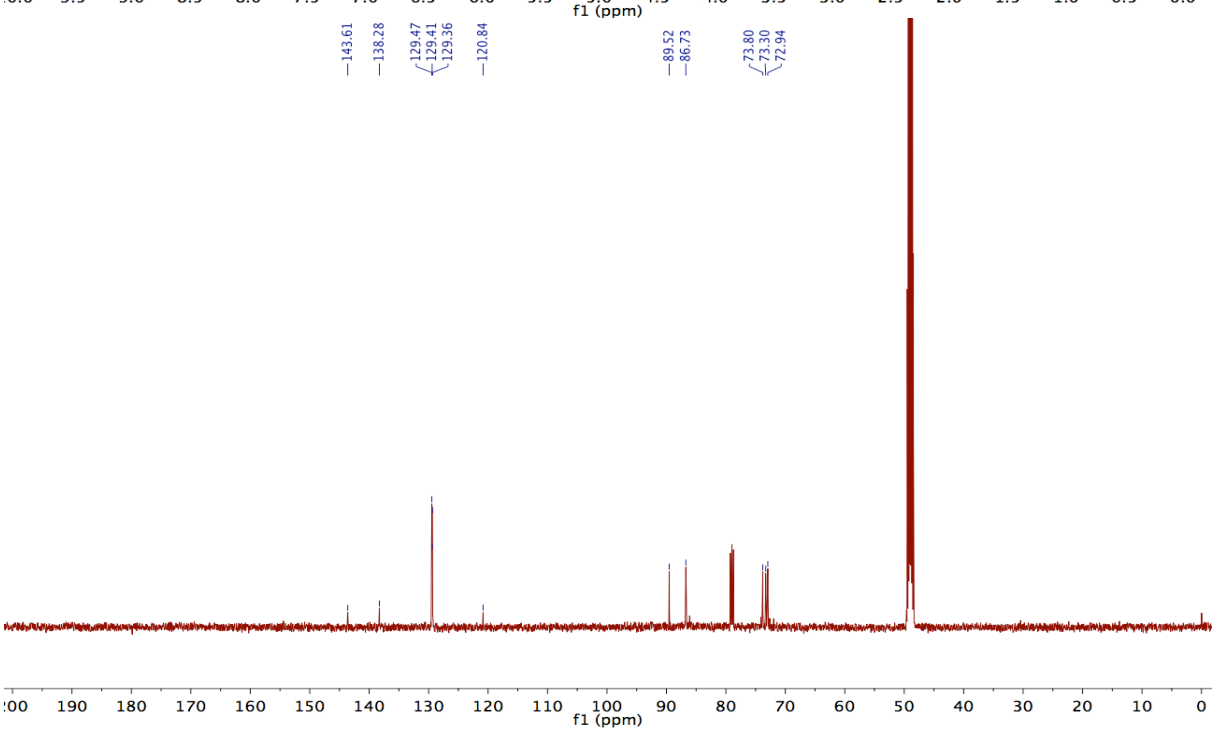
143.61
138.28
129.47
129.41
129.36
120.84
89.52
86.73
73.80
73.30
72.94
f1 (ppm)

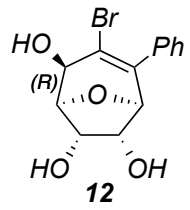
Br
HO
Ph
(R)
O
HO
OH

12

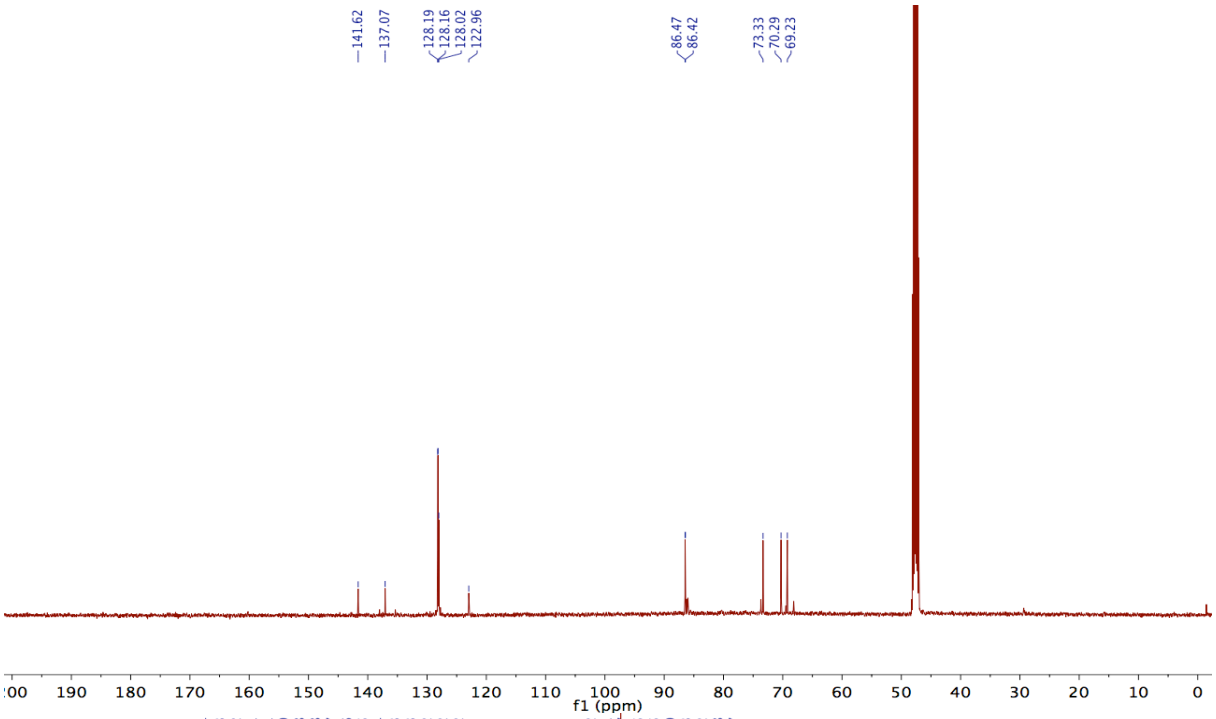
141.62
137.07
128.19
128.16
128.02
122.96
86.47
86.42
73.33
70.29
69.23
f1 (ppm)

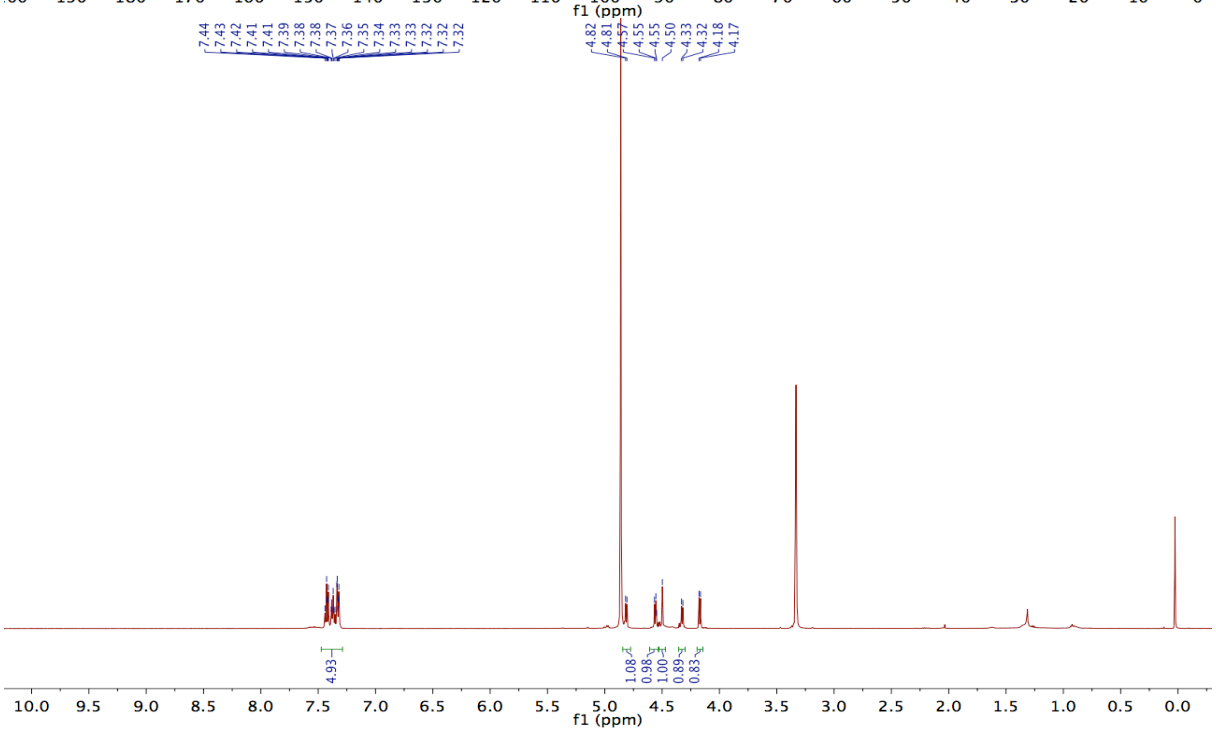
7.44
7.43
7.42
7.41
7.41
7.39
7.38
7.38
7.37
7.36
7.35
7.34
7.33
7.33
7.32
7.32
7.32
4.82
4.81
4.57
4.55
4.55
4.50
4.33
4.32
4.18
4.17
4.93
1.08
0.98
1.00
0.89
0.83
f1 (ppm)

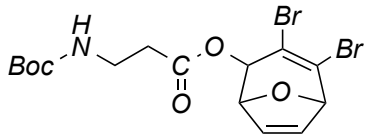
H
N
Boc
C
O
O
O
Br
Br

13

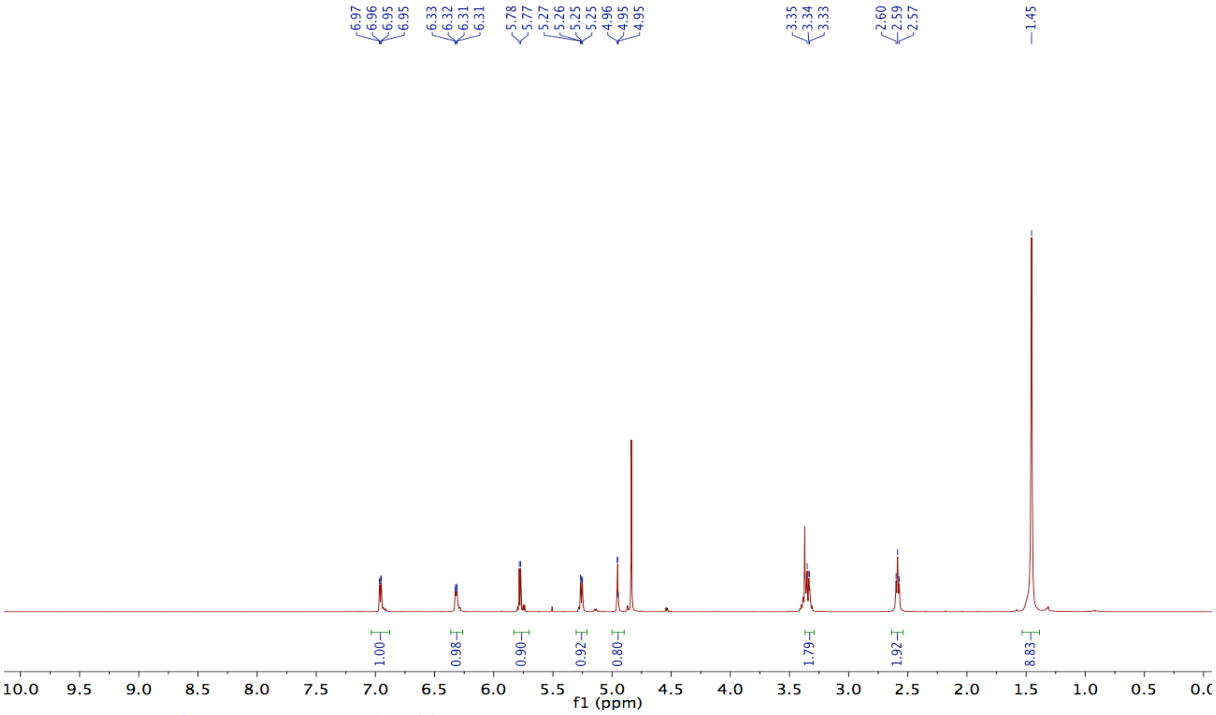
6.97
6.96
6.95
6.95
6.33
6.32
6.31
6.31
5.78
5.77
5.27
5.26
5.25
5.25
4.96
4.95
4.95
3.35
3.34
3.33
2.60
2.59
2.57
1.45
1.00
0.98
0.90
0.92
0.80
1.79
1.92
8.83
f1 (ppm)

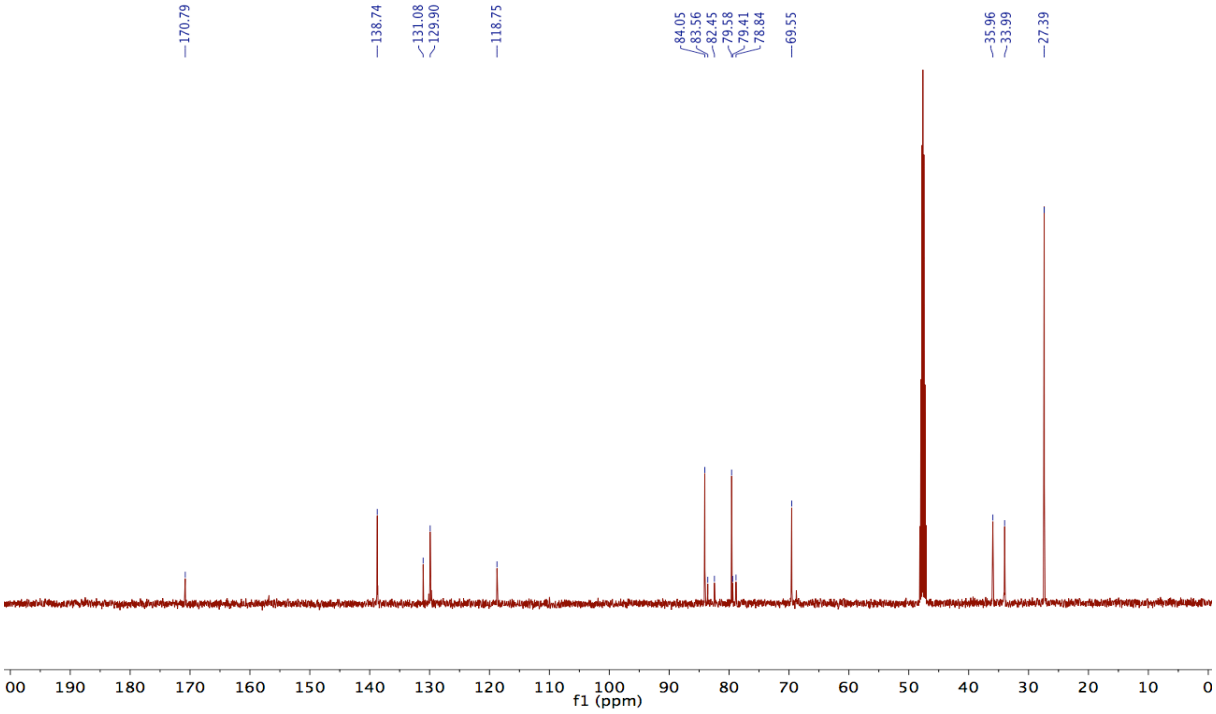
170.79
138.74
131.08
129.90
118.75
84.05
83.56
82.45
79.58
79.41
78.84
69.55
35.96
33.99
27.39
f1 (ppm)

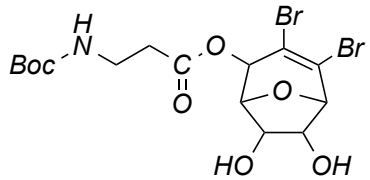
H
N
Boc
C
O
O
O
Br
Br
HO
OH

14

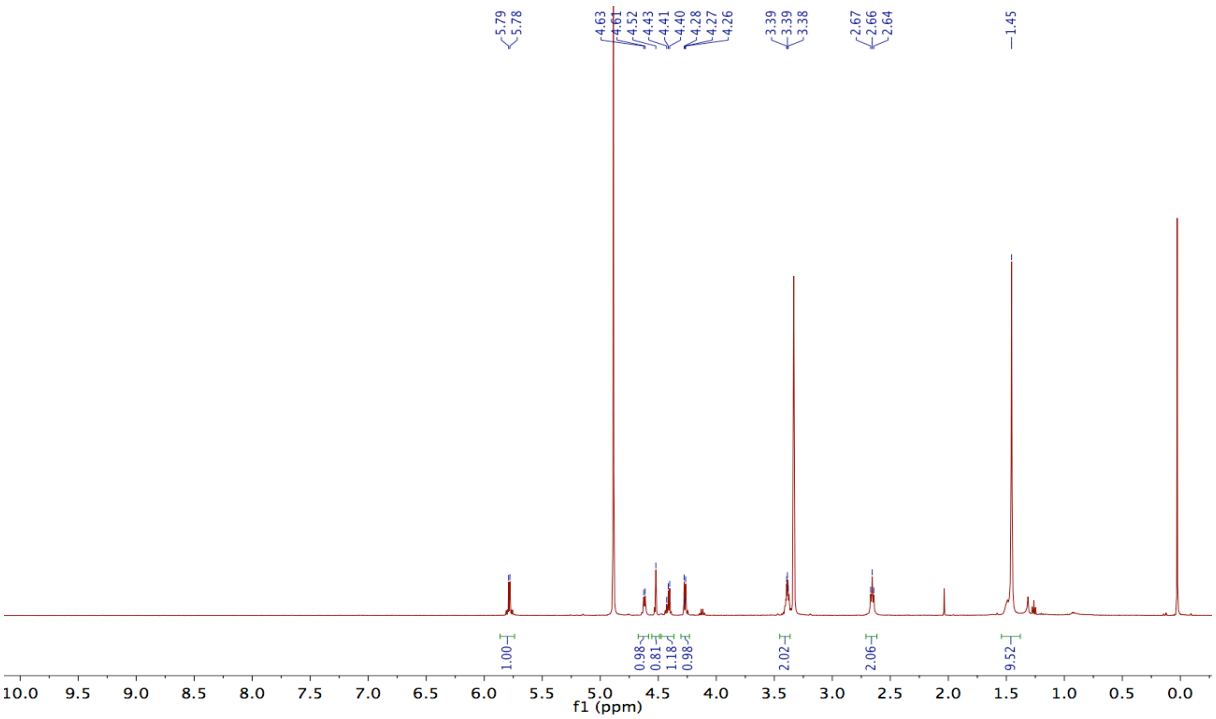
5.79
5.78
4.63
4.61
4.52
4.43
4.41
4.40
4.28
4.27
4.26
3.39
3.39
3.38
2.67
2.66
2.64
1.45
1.00
0.98
0.81
1.18
0.98
2.02
2.06
9.52
f1 (ppm)

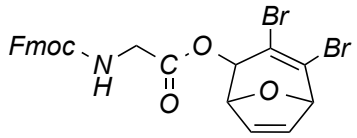
Fmoc
N
H
C
O
O
Br
Br
O

16

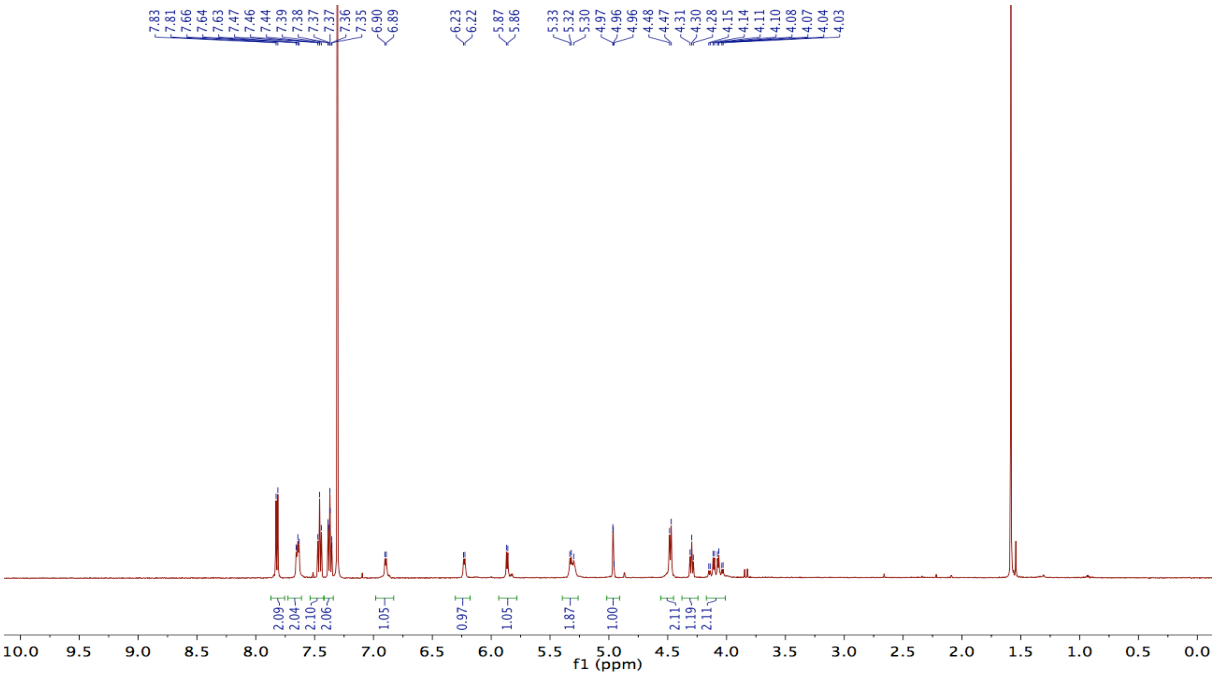
7.83
7.81
7.66
7.64
7.63
7.47
7.46
7.44
7.39
7.38
7.37
7.37
7.36
7.35
6.90
6.89
6.23
6.22
5.87
5.86
5.33
5.32
5.30
4.97
4.96
4.96
4.48
4.47
4.31
4.30
4.28
4.15
4.14
4.11
4.10
4.08
4.07
4.04
4.03
2.09
2.04
2.10
2.06
1.05
0.97
1.05
1.87
1.00
2.11
1.19
2.11
f1 (ppm)

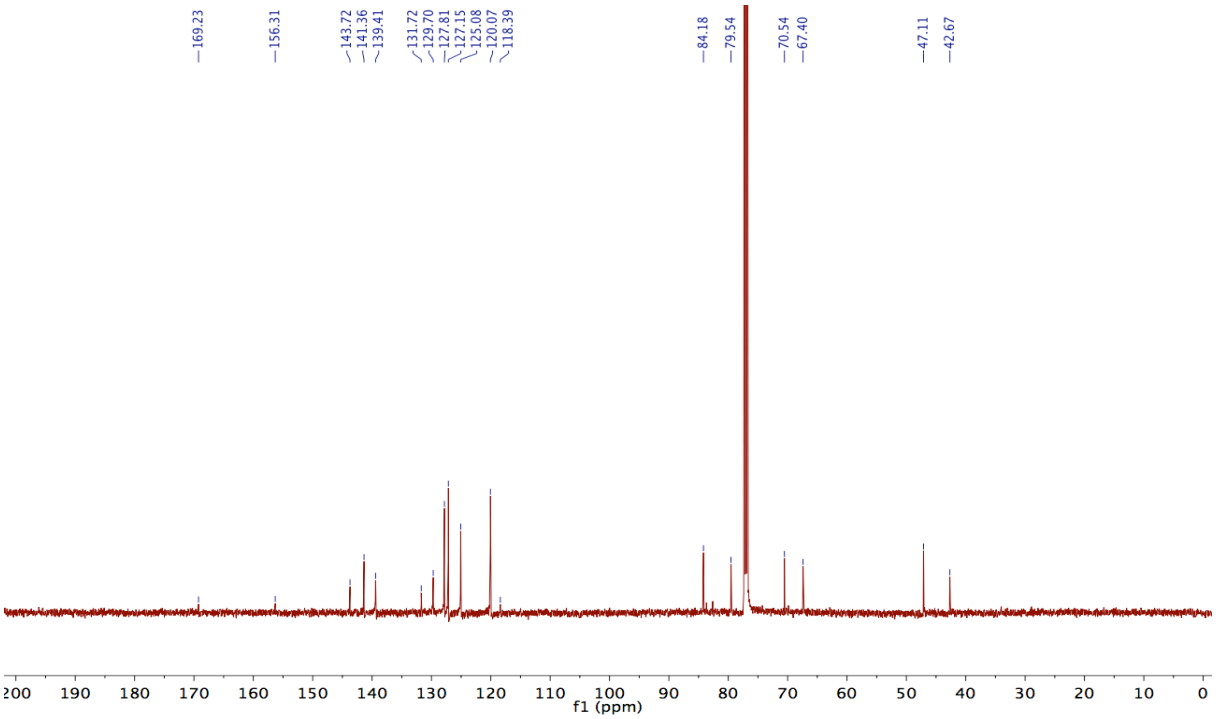
169.23
156.31
143.72
141.36
139.41
131.72
129.70
127.81
127.15
125.08
120.07
118.39
84.18
79.54
70.54
67.40
47.11
42.67
f1 (ppm)

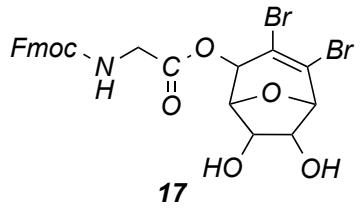
Fmoc
N
H
C
O
O
Br
Br
O
HO
OH

17

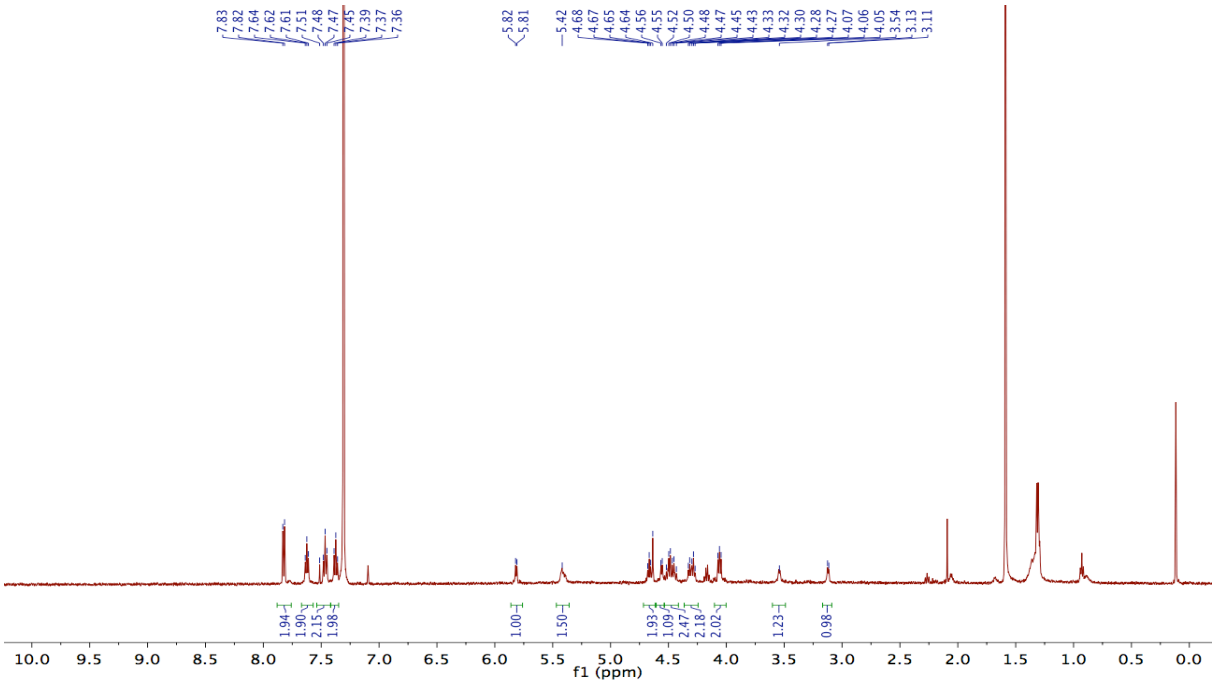
7.83
7.82
7.64
7.62
7.61
7.51
7.48
7.47
7.45
7.39
7.37
7.36
5.82
5.81
5.42
4.68
4.67
4.65
4.64
4.56
4.55
4.52
4.50
4.48
4.47
4.45
4.43
4.33
4.32
4.30
4.28
4.27
4.07
4.06
4.05
3.54
3.13
3.11
1.94
1.90
2.15
1.98
1.00
1.50
1.93
1.09
2.47
2.18
2.02
1.23
0.98
f1 (ppm)

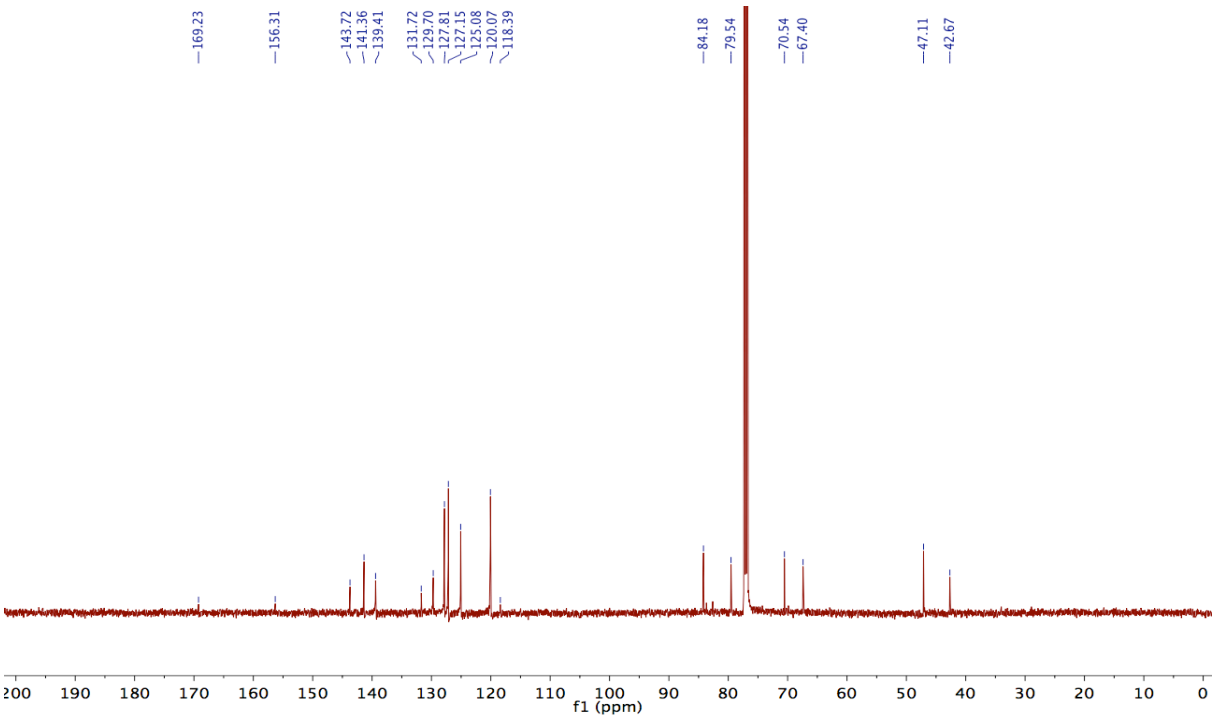
169.23
156.31
143.72
141.36
139.41
131.72
129.70
127.81
127.15
125.08
120.07
118.39
84.18
79.54
70.54
67.40
47.11
42.67
f1 (ppm)